AGU100 ADVANCING EARTH AND SPACE SCIENCE

JGR

Journal of Geophysical Research: Planets

RESEARCH ARTICLE
10.1029/2018JE005710

Key Points:
- Episodic fluvial processes occurred in the southwest Melas basin, Valles Marineris, Mars, likely during the Hesperian period
- Evidence for multiple "wet and dry" periods is preserved in the fluvial systems and paleolacustrine deposits
- Local Valles Marineris climate likely supported runoff and precipitation and transitioned from perennial to ephemeral conditions

Supporting Information:
- Supporting Information S1

Correspondence to:
J. M. Davis,
joel.davis@nhm.ac.uk

Citation:
Davis, J. M., Grindrod, P. M., Fawdon, P., Williams, R. M. E., Gupta, S., & Balme, M. (2018). Episodic and declining fluvial processes in southwest Melas Chasma, Valles Marineris, Mars. *Journal of Geophysical Research: Planets, 123*, 2527–2549. https://doi.org/10.1029/2018JE005710

Received 4 JUN 2018
Accepted 20 AUG 2018
Accepted article online 29 AUG 2018
Published online 8 OCT 2018

Author Contributions:
Conceptualization: J. M. Davis
Data curation: J. M. Davis
Formal analysis: J. M. Davis
Investigation: J. M. Davis, P. M. Grindrod, P. Fawdon, R. M. E. Williams, S. Gupta, M. Balme
Methodology: J. M. Davis
Supervision: P. M. Grindrod, S. Gupta, M. Balme
Visualization: J. M. Davis, P. Fawdon
Writing - original draft: J. M. Davis
Writing – review & editing: J. M. Davis, P. M. Grindrod, P. Fawdon, R. M. E. Williams, S. Gupta, M. Balme

Episodic and Declining Fluvial Processes in Southwest Melas Chasma, Valles Marineris, Mars

J. M. Davis[1], P. M. Grindrod[1], P. Fawdon[2], R. M. E. Williams[3], S. Gupta[4], and M. Balme[2]

[1]Department of Earth Sciences, Natural History Museum, London, UK, [2]School of Physical Sciences, The Open University, Milton Keynes, Buckinghamshire, UK, [3]Planetary Science Institute, Tucson, AZ, USA, [4]Department of Earth Sciences and Engineering, Imperial College London, London, UK

Abstract There is abundant evidence for aqueous processes on Noachian terrains across Mars; however, key questions remain about whether these processes continued into the Hesperian as the martian climate became less temperate. One region with an extensive Hesperian sedimentary record is Valles Marineris. We use high-resolution image and topographic data sets to investigate the fluvial systems in the southwest Melas basin, Valles Marineris, Mars. Fluvial landforms in the basin exist across a wide area, and some are preserved as inverted channels. The stratigraphy of the basin is complex: Fluvial landforms are preserved as planview geomorphic features and are also interbedded with layered deposits in the basin. The fluvial morphologies are consistent with formation by precipitation-driven runoff. Fluvial processes in the basin were episodic, suggesting multiple wet and dry periods. During dry periods, mantling material accumulated, and significant volumes of sediment were eroded, inverting fluvial channels. During wet periods, inverted channels and mantling material infilling valleys were incised by further fluvial erosion. These trends for episodic fluvial processes are similarly reflected in the central depression of the southwest Melas basin, previously described as a paleolake. Ultimately, fluvial processes in the basin gradually shut down, becoming geographically restricted, and then ceased entirely. We show that branching valley networks are also present on the plateaus above Melas and Ius Chasma, which converge on the heads of tributary canyons. These suggest that precipitation-driven runoff processes also extended onto the plateaus of Valles Marineris.

Plain Language Summary There is strong evidence that liquid water was widespread on ancient Mars (prior to 3.7 billion years ago), and features such as rivers and lakes were common. However, it is unclear how Mars changed from this relatively wet state to the cold and dry planet we see today. Using high-resolution satellite images, we investigate part of the canyon system Valles Marineris, near the equator. This region of Valles Marineris, the southwest Melas basin, forms a depression and contains sediments and landforms that are from this middle period of Mars' history. We examined both the sediments and landforms and found that they most likely formed due to the presence of river valleys and channels and lakes. We find that the southwest Melas basin had repeated wet and dry periods, when the rivers and lakes dried up, before later refilling. During this time, hundreds of meters of sediment was deposited and eroded in the basin. This wet and dry cycle repeated several times, before ultimately ceasing. We also find that river valleys were present on the plateaus of Valles Marineris, above the basin. Our results suggest that liquid water persisted after 3.7 billion years ago, at least locally on this part of Mars.

1. Introduction

Much of early Mars was modified by liquid water, evidence of which is preserved in widespread erosional and depositional landforms across its surface. Many Noachian-aged (>3.7 Ga; Hartmann & Neukum, 2001; Michael, 2013) surfaces contain valley and channel networks (e.g., Carr, 1995; Craddock & Howard, 2002; Hynek et al., 2010; Hynek & Phillips, 2003; Irwin & Howard, 2002), degraded craters consistent with fluvial erosion (e.g., Craddock et al., 1997; Howard et al., 2005), paleolake basins (e.g., Fassett & Head III, 2008b; Goudge, Fassett, et al., 2016), and sedimentary fan deposits, interpreted as both alluvial (e.g., Kraal et al., 2008; Moore et al., 2003; Moore & Howard, 2005) and deltaic systems (e.g., Di Achille & Hynek, 2010; Goudge, Milliken, et al., 2016; Malin & Edgett, 2003; Rice et al., 2013). Extensive deposits of hydrated minerals, such as phyllosilicates (e.g., Bibring et al., 2006; Ehlmann & Edwards, 2014), are also present across Noachian terrains, providing further evidence that the Noachian was a period of widespread aqueous alteration.

Globally, linked fluvial-lacustrine systems appear concentrated on late Noachian terrains and are considered to have been active near the Noachian/Hesperian (Hesperian; ~3.7–3.0 Ga; Hartmann & Neukum, 2001; Michael, 2013) boundary, pointing to an intense period of fluvial activity around this time (Fassett & Head III, 2008a; Howard et al., 2005; Irwin, Howard, et al., 2005), possibly supported by a multibar CO_2 atmosphere (Jakosky et al., 2017). This climate optimum was followed by a decline in conditions favorable to liquid water, as the atmosphere was lost to space and the martian environment began to transition to a cold, hyperarid desert (Jakosky et al., 2017). Evidence for a decline in fluvial processes during the Hesperian (Fassett & Head III, 2008a; Howard et al., 2005; Irwin, Howard, et al., 2005) includes numerous laterally expansive, large igneous provinces of Hesperian age, which have not been dissected by fluvial activity (Tanaka et al., 2014). However, exactly how rapidly the martian environment changed, and whether this was a rapid global change or varied regionally remains unclear. Indeed, there are a growing number of reported Hesperian and younger surfaces that have been extensively modified by long-lived aqueous processes (e.g., at Gale Crater; Grotzinger et al., 2015; Rice et al., 2017; Williams et al., 2013), particularly in equatorial regions (e.g., Burr et al., 2010; Grindrod et al., 2012, 2017; Goddard et al., 2014; Le Deit et al., 2010; Mangold et al., 2004, 2008; Salese et al., 2016; Weitz et al., 2008, 2010). These modified surfaces mean that the period that conditions were favorable to liquid water on Mars potentially persisted beyond the Noachian, at least at a local or regional scale.

One of these regions is Valles Marineris, Mars' equatorial canyon system, which contains an extensive record of sedimentary deposits within its multiple troughs. The formation and development of Valles Marineris is protracted, extending from the late Noachian to early Amazonian (e.g., Anderson et al., 2001; Andrews-Hanna, 2012; Schultz, 1991; Warner et al., 2013; Witbeck et al., 1991), and thus, its sedimentary deposits predominantly record the nature of Hesperian environmental conditions. The formation of Valles Marineris is associated with both the emplacement of Tharsis to the west and the resulting structural collapse (e.g., Anderson et al., 2001; Andrews-Hanna, 2012), and the circum-Chryse outflow channels to the east, largely thought to have formed by catastrophic floods, which may have originated in Valles Marineris (e.g., Rotto & Tanaka, 1995; Warner et al., 2013).

Valles Marineris shows strong geomorphic and mineralogical evidence that the canyons have been extensively modified by aqueous processes during the Hesperian and Amazonian. Fluvial erosional systems are found across multiple plateaus above the canyons and along the canyon walls (Le Deit et al., 2010; Mangold et al., 2004, 2008; Quantin et al., 2005; Singh et al., 2017; Weitz et al., 2008, 2010). Deposits of hydrated minerals (e.g., suites of clays and sulfates) are also found along the Valles Marineris plateaus (Le Deit et al., 2010; Weitz et al., 2010) and within the chasmata (e.g., Liu & Catalano, 2016; Murchie et al., 2009; Roach et al., 2010; Weitz et al., 2015). Fans interpreted to be alluvial and deltaic are found in Melas Chasma (e.g., Metz et al., 2009; Williams & Weitz, 2014) and Coprates Chasma, which also display a hydrated mineralogy (Grindrod et al., 2017; Weitz & Bishop, 2016). Hydrological modeling has predicted the emergence of regional groundwater throughout Valles Marineris (e.g., Andrews-Hanna et al., 2010). Numerous sedimentary mounds, present within multiple Valles Marineris troughs, are known as interior layered deposits (Chapman & Tanaka, 2001) and have been associated with an influx of groundwater (e.g., Grindrod & Balme, 2010; Murchie et al., 2009), the trapping and weathering of snow/ice deposits (e.g., Michalski & Niles, 2012), or the evaporation of large bodies of water (e.g., Gendrin et al., 2005). The aqueous history of Valles Marineris is thus both diverse and complex, but despite much study, it is still unclear whether the Valles Marineris troughs were once host to a large standing body of water (e.g., Andrews-Hanna, 2012; Lucchitta, 2010).

In this study, we investigate the southwest Melas basin (SMB) within Valles Marineris (Figure 1). Erosional fluvial valley networks are present throughout the SMB, some of which converge on a well-defined depression (e.g., Quantin et al., 2005; Williams & Weitz, 2014). This depression contains a succession of well-preserved deposits interpreted as deltaic and lacustrine (e.g., Metz et al., 2009; Williams & Weitz, 2014), strong evidence that the SMB once hosted a lake. Recent work on these paleolake deposits has suggested that this lake may have drained before later refilling (Williams & Weitz, 2014), indicating that aqueous processes in the SMB may have been episodic. Excellent High Resolution Imaging Science Experiment (HiRISE; 0.25 m per pixel; McEwen et al., 2007) coverage means that the geology of the entire source to sink sequence can now be studied at high resolution across nearly all of the basin. Given that the paleolake contains evidence for different paleo-environments and at least one regression (Figure 2 and supporting information Figures S1–S3), evidence for the landscape response to environmental change and episodic processes may be recorded in

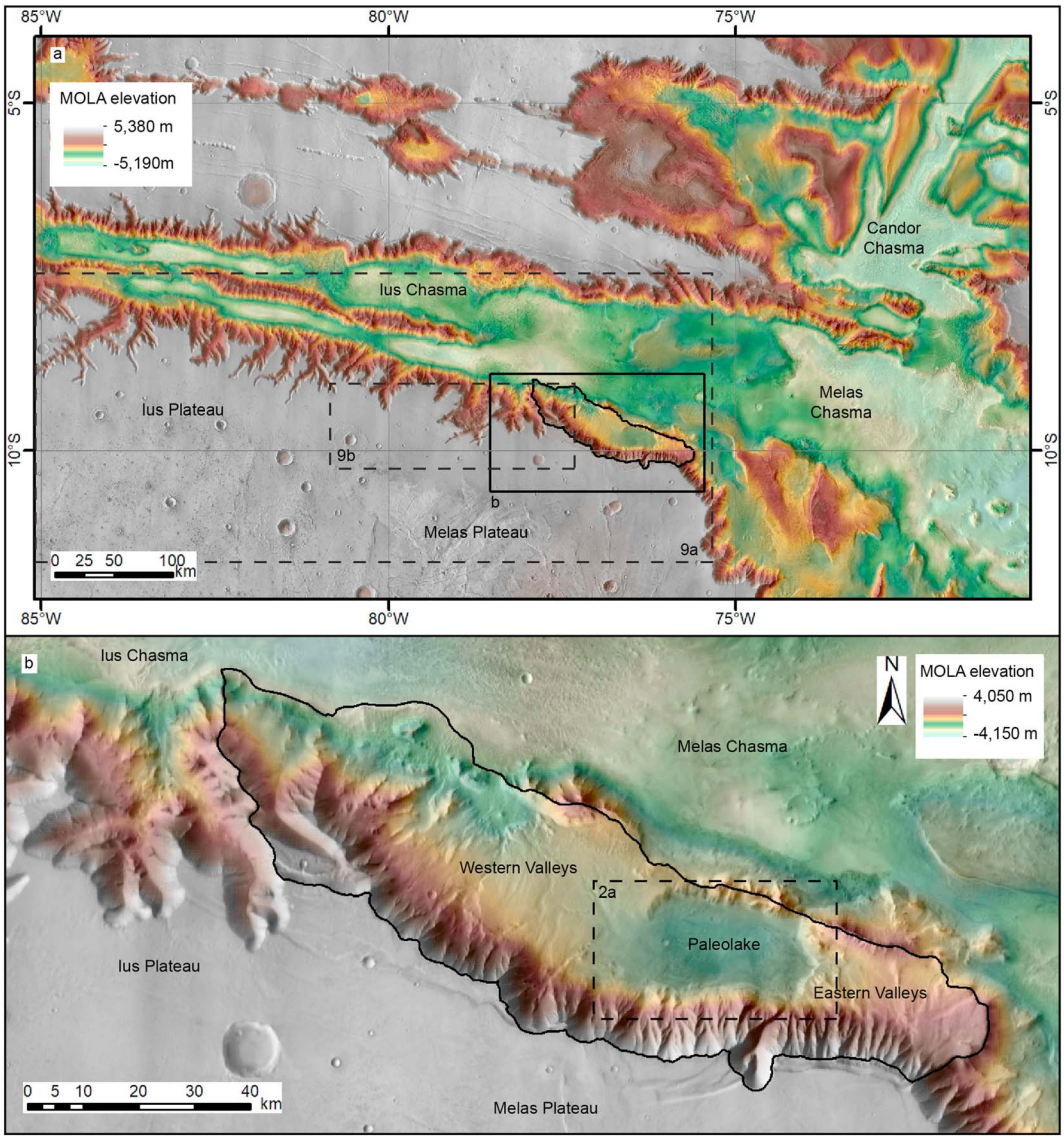

Figure 1. (a) Central and western parts of Valles Marineris. The southwest Melas basin (SMB) is shown by the black solid outline. (b) Enlarged view of the SMB. Valleys and channels converge on the SMB paleolake from the west and the east of the basin. The study area where fluvial systems were systematically mapped is shown by the black outline. Both images show MOLA (Mars Orbital Laser Altimeter) topography overlaid on a Thermal Emission Imaging System-infrared daytime (Christensen et al., 2004) basemap. (Note that all image numbers shown in figures are listed in the supporting information).

the fluvial systems of the SMB catchment. To look for such evidence, we use high-resolution imagery and topographic data sets to investigate the fluvial systems found within the basin's catchment; our comprehensive use of HiRISE data separates this study from previous work. We describe their geomorphology and use stratigraphic relationships to tie the fluvial evolution of the catchment to the paleolake deposits. We also investigate the Valles Marineris plateaus above the SMB for evidence of regional fluvial processes and how those may relate to the basin. Finally, we apply our results to consider the nature of the Hesperian climate in this region of Valles Marineris.

2. Background to the SMB

Our study area is the SMB, an enclosed basin in Melas Chasma, the central trough in Valles Marineris (Figure 1). Erosional landforms and exhumed deposits of the basin stratigraphy record a spectrum of aqueous processes (Dromart et al., 2007; Mangold et al., 2004; Metz et al., 2009; Quantin et al., 2005; Williams & Weitz,

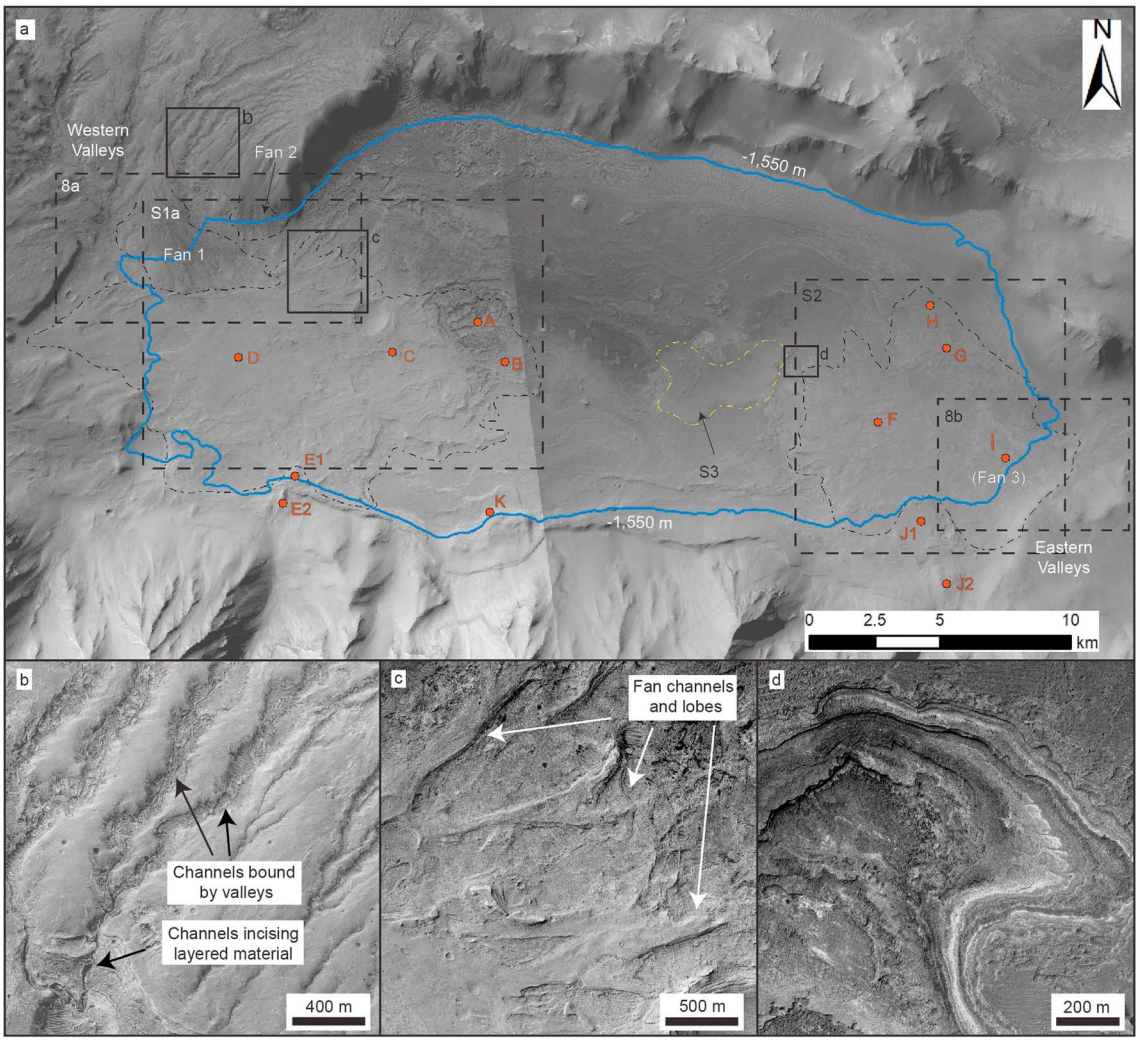

Figure 2. (a) Context Camera mosaic of paleolake in the southwest Melas basin, which was fed by fluvial systems from its western and eastern edges. The black dashed lines show the western and eastern fan complexes, and Fans 1 and 2 (described later); the yellow dashed line shows the extent of the indurated eolian bedforms; red dots show individual sedimentary fans as defined by Williams and Weitz (2014); the blue line shows a shoreline at −1,550 m (extracted from a High Resolution Stereo Camera digital elevation model) inferred from the fan apexes by Williams and Weitz (2014); (b) High Resolution Imaging Science Experiment (HiRISE) image of fluvial valleys and channels incising into layered deposits at the western edge of the paleolake; (c) HiRISE image of inverted channel and lobate fan deposits in the western fan complex; (d) HiRISE image of layered deposits, interpreted as lacustrine, which vary in texture, brightness, and erosional profile.

2014). Central to this interpretation are erosional fluvial valley networks and paleolake deposits in a depression (herein referred to as the *paleolake*) in the east of the basin (Figure 2; Dromart et al., 2007; Mangold et al., 2004; Metz et al., 2009; Quantin et al., 2005; Williams & Weitz, 2014). Impact crater size-frequency distribution data from the basin suggest these processes occurred in the Hesperian period, after the initial formation phase of Valles Marineris (~3.5 Ga; Quantin et al., 2005), likely postdating the global valley-forming phase at the Noachian/Hesperian boundary (e.g., Fassett & Head III, 2008a; Irwin, Howard, et al., 2005).

Extensive networks of branching, erosional valleys and channels feed into the western end of the paleolake. A more poorly preserved network of erosional valleys and channels drains into the eastern side of the paleolake, indicating that the basin hosted geographically diverse surface fluvial pathways (Figure 1b; Mangold et al., 2004; Quantin et al., 2005). The paleolake is defined by both the modern topographic relief and exhumed deposits bound by the depression. The lack of any outlet valleys or channels indicates that the paleolake was a closed basin system (e.g., Fassett & Head III, 2008b). The complex range of exhumed deposits within the paleolake (interbedded deltaic and lacustrine deposits) is consistent with the paleolake holding

water for sustained periods of time (10^2–10^5 years; Metz et al., 2009; Quantin et al., 2005; Williams & Weitz, 2014), rather than being a purely alluvial or ephemeral system.

Branching, erosional fluvial valleys and channels appear concentrated to the west of the paleolake (Figure 2), and originate from a range of elevations, and hence are interpreted to have formed due to precipitation and runoff (Mangold et al., 2004; Quantin et al., 2005; Williams & Weitz, 2014). These fluvial systems incise a medium-toned, layered, draping material, which is spectrally bland (Le Deit et al., 2010; Quantin et al., 2005; Weitz et al., 2015). Overlying this material and infilling the valleys is a lighter toned, layered draping material, which contains a suite of hydrated minerals, such as hydrated silica and sulfates, and does not appear to be dissected by erosional valleys (these materials are referred to as *ML* and *LD*, respectively, by Weitz et al. (2015)). Both ML and LD are interpreted as volcanic ash or atmospheric dust deposits, which have been subject to some degree of chemical weathering (Weitz et al., 2015), which is broadly consistent with the geomorphology.

In a comprehensive study of the paleolake succession, Williams and Weitz (2014) identified 13 fan structures (labeled Fans A–K; see Figures 2, S1, and S2), interpreted as a combination of alluvial fans, fan deltas, deltas, deep subaqueous fans, debris fans, and landslides. Many of these fan structures are interfingered with laterally extensive layered deposits, which vary in brightness and erosional profile, and are interpreted as forming in a lacustrine setting (Quantin et al., 2005; Williams & Weitz, 2014). The distribution of sediment fans suggests that the water level extended up to at least ~−1,550 m (relative to Mars Orbital Laser Altimeter [MOLA]; Smith et al., 2001; Zuber et al., 1992) aeroid; Williams & Weitz, 2014), giving a maximum lake depth of ~400 m. Midway up the succession of lacustrine deposits, a series of indurated bedforms has been exposed by erosion, which are comparable to cemented Transverse Aeolian Ridges (e.g., Balme et al., 2008), which form subaerially (Figure S3; Williams & Weitz, 2014). As the surface on which these bedforms occur is stratigraphically bound by lacustrine deposits, the bedforms indicate a period of lake-level regression in which the lacustrine deposits were subaerially exposed, before the water level rose again (Williams & Weitz, 2014).

The SMB paleolake deposits thus contain evidence for a variety of different subaerial, near shore, and deep water environments. While other ancient sedimentary basins with similarly developed valley networks and sedimentary fan features exist elsewhere on Mars (e.g., Di Achille & Hynek, 2010; Goudge, Milliken, et al., 2016; Rice et al., 2013), few Hesperian basins exist with such a well-preserved stratigraphy. Thus, the SMB is an ideal location to investigate the nature of Hesperian aqueous processes. For these reasons, the basin was considered as a landing site for the Mars Exploration Rovers (Weitz et al., 2003), Mars Science Laboratory (Quantin et al., 2006), and the Mars 2020 Rover missions (Davis et al., 2017; Williams et al., 2014, 2015).

3. Data and Methods

We used a combination of meter and submeter resolution Context Camera (CTX; ~6 m per pixel; Malin et al., 2007) and HiRISE (McEwen et al., 2007) data sets for this study. We defined our main study area within the SMB using the topographic barriers surrounding the basin and recognizable in MOLA topographic data (Figure 1). The Valles Marineris main canyon wall formed the southern boundary of the study area, and a NW-SE trending topographic rise formed the northern boundary. We mapped all fluvial features (i.e., erosional valley and channel networks and depositional channels) that we considered part of the catchment within this study area (Figure 1b). These fluvial landforms were primarily mapped using the near continuous HiRISE (digitized at ~1:2,000 scale; Figure S4) and CTX data (digitized at ~1:10,000 scale), where HiRISE were not available. We also mapped fluvial systems on the Valles Marineris plateau adjacent to the SMB, using CTX data only, because there is sparse HiRISE coverage here. Fluvial characteristics, such as drainage density, stream order, channel/valley width and depth, and sinuosity, were calculated and recorded wherever possible. Drainage densities for the drainage networks were calculated by dividing the cumulative length of fluvial systems by the total drainage area.

We produced HiRISE and CTX digital elevation models (DEMs; Tables S1 and S2 and Figure S5) using the U.S. Geological Survey Integrated Software for Imagers and Spectrometers software and the BAE photogrammetric package SOCET SET (Kirk et al., 2008). The DEMs were produced with a post spacing of 1 and 20 m per pixel for HiRISE and CTX, respectively. The DEMs were used to identify watersheds and drainage directions of the fluvial systems in the catchment and to measure their elevation ranges. In the absence of

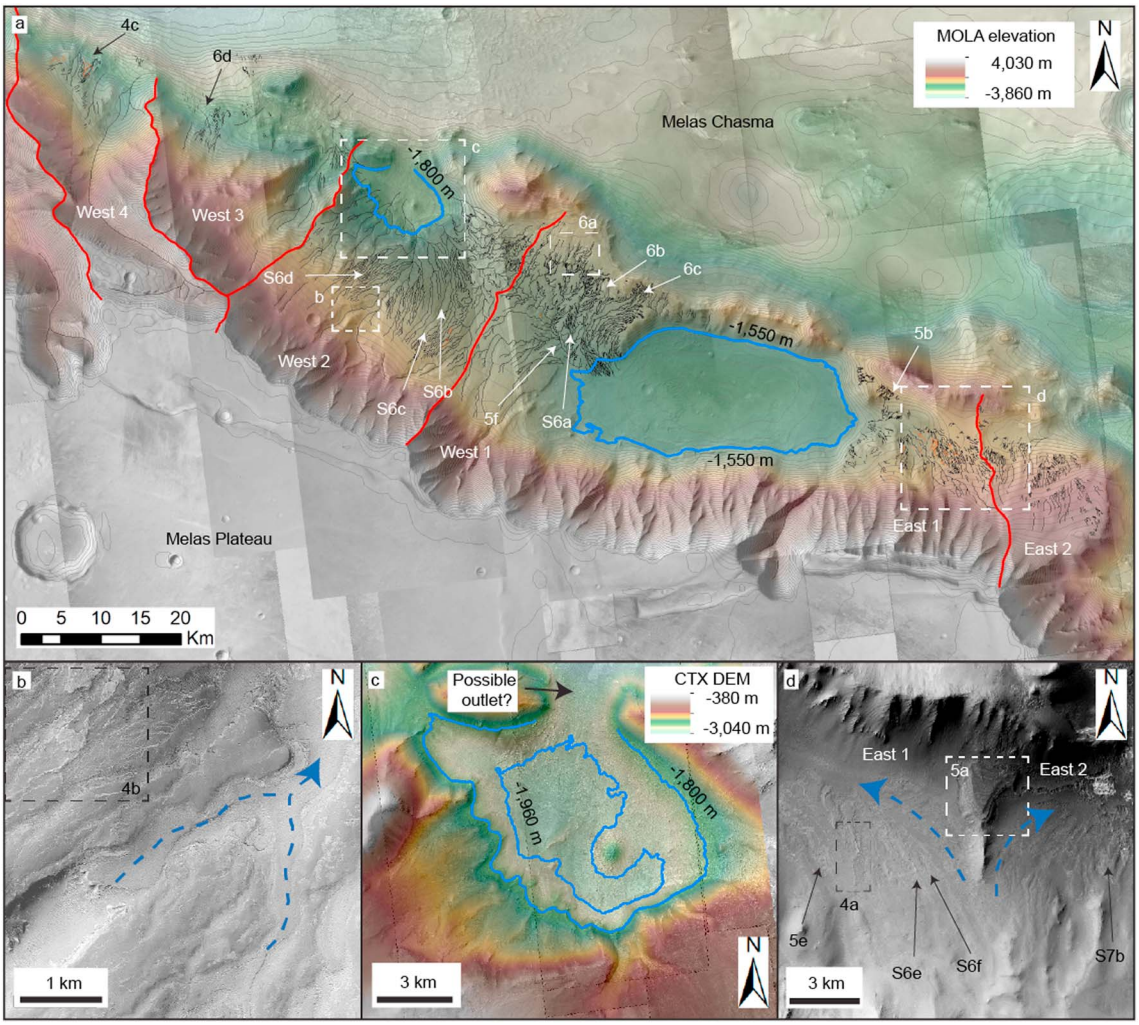

Figure 3. (a) Map of fluvial landforms in the southwest Melas basin on a background of MOLA topography overlaid on a CTX mosaic and THEMIS-IR daytime basemap (contours have 100 m spacing). Valley networks and channels systems are shown by the black lines; inverted channels are shown by orange lines. The basin has been divided into six drainage networks separated by watersheds (red lines). Putative shorelines for the central paleolake (Quantin et al., 2005) and the western paleolake are shown by the blue lines. (b) HiRISE image of valley networks and channel systems in the West 2 drainage network. (c) CTX DEM (digital elevation model) of the western paleolake, overlaid on a basemap of HiRISE and CTX images. The West 2 fluvial systems converge on the paleolake from the south. A fully enclosed depression forms at −1,960 m, and a near enclosed depression forms at −1,800 m. A possible outlet for the paleolake exists at its northern end, leading into the main Melas Chasma trough. (d) CTX image of the East 1 and 2 drainage networks, which drain into the central paleolake and the main Melas Chasma trough, respectively. Blue arrows show the downslope direction.

HiRISE or CTX DEM coverage, High Resolution Stereo Camera (Neukum & Jaumann, 2004) DEMs (50 m per pixel; Jaumann et al., 2007) and MOLA data were used to determine topographic information. Hyperspectral data sets from the Compact Reconnaissance Imaging Spectrometer for Mars (Murchie et al., 2009) of the SMB have already been extensively studied, which found few detections of hydrated minerals within the basin (e.g., Weitz et al., 2010, 2015).

4. Observations

4.1. Mapping and Distribution of the Catchment Landforms

To reconstruct the history of the SMB, we mapped all landforms in the basin's catchment that we considered fluvial. In this section, we first describe the identification and distribution of the fluvial landforms exposed in the basin catchment, which are abundant throughout the SMB (Figure 3). Although erosional valley and

Table 1
Characteristics of the Fluvial Systems Within the SMB Catchment

Drainage network	Fluvial landforms	Width (m)	Depth[a] (m)	Planview morphology observed	Max. stream order	Max. sinuosity	Drainage density (km^{-1})
West 4	Valleys, channels, and inverted channels	Valleys: 500–800 Channels: 20–150 Inverted channels: 10–30	Valleys: 50–200 Channels: 5–10 Inverted channels: 5–20	Subdendritic to subparallel	4	1.07	0.24
West 3	Valleys and channels	Valleys: 300–600 Channels: 20–150	Valleys: 50–250 Channels: 5–20	Subdendritic to subparallel	4	1.08	0.22
West 2	Valleys, channels, and inverted channels	Valleys: 300–1000 Channels: 20–100 Inverted channels: 10–50	Valleys: 30–150 Channels: 5–20 Inverted channels: 5–10	Mostly dendritic to subparallel; some meandering	8	1.30	1.97
West 1	Valleys, channels, and inverted channels	Valleys: 300–750 Channels: 10–60 Inverted channels: 10–50	Valleys: 20–80 Channels: 5–20 Inverted channels: <5 m	Mostly dendritic to subparallel; some meandering	8	1.39	1.42
East 1	Valleys, channels, and inverted channels	Valleys: 200–800 Channels: 20–100 Inverted channels: 10–50	Valleys: 20–80 Channels: 5 Inverted channels: 5–10	Subdendritic to parellel	5	1.13	0.68
East 2	Valleys, channels, and inverted channels	Valleys: 200–800 Channels: 20–100 Inverted channels: 5–20	Valleys: 20–80 Channels: 5 Inverted channels: 10–20	Subparallel to parallel	5	1.17	1.34

Note. Morphologies are after Zernitz (1932).
[a]Values for inverted channels are heights, not depths.

channel networks are best preserved adjacent to the paleolake (Quantin et al., 2005; Williams & Weitz, 2014), our observations show that fluvial systems are common across the entire SMB (note that we use the term *fluvial system* to refer to the catchment landforms and not the sediment fans within the adjacent paleolake). The inferred drainage patterns of these systems are not simple, and the fluvial systems originate and terminate at a wide range of elevations; the lowest-order stream of many of the fluvial systems extend up to the local drainage divides (Figure 3). The fluvial systems have extensively modified the landscape within the basin, as indicated by the eroded topography (Figures 3–6 and S6). Based upon topographic barriers within the SMB, we have divided the fluvial systems in the catchment into six drainage networks (Figure 3 and Table S3). West to east, these are as follows: West 4–1 and East 1–2. The drainage direction of these systems was determined using a combination of topographic slope and the characteristics of the fluvial systems (e.g., downstream changes in width or depth, convergence directions of tributary branches).

4.2. Morphology of the Catchment Landforms

Here we describe the morphology and characteristics of the different landforms identified in the catchment, which we considered fluvial. Both erosional valleys and interior channels were identified in all six of the drainage networks (Figures 3 and S6). The erosional valleys and channels range in width from tens to hundreds of meters (Table 1) and are contiguous for up to tens of kilometers. Erosional valleys are up to ~250 m deep and channels are typically ~5–20 m deep. Well-preserved erosional valleys often contain interior channels; however, many other channels are not valley bound (Figures 3 and S6). Other erosional valleys do not contain channels, although these valleys appear to correlate to locations where they have been modified by later burial and/or erosion, possibly obscuring any channels from detection. The erosional valleys adjacent to the southern Valles Marineris wall are buried by younger mass wasting deposits into the basin.

Drainage densities for the fluvial systems in the catchment range from 0.22 to 1.97 km^{-1} (Tables 1 and S4). Drainage densities are highest for the West 1 and 2 drainage networks and lowest for the West 3 and 4 drainage networks. East 1 and 2 have a particularly high concentration of fluvial systems when compared to previous studies (e.g., Quantin et al., 2005). All drainage networks have Strahler stream orders of at least four

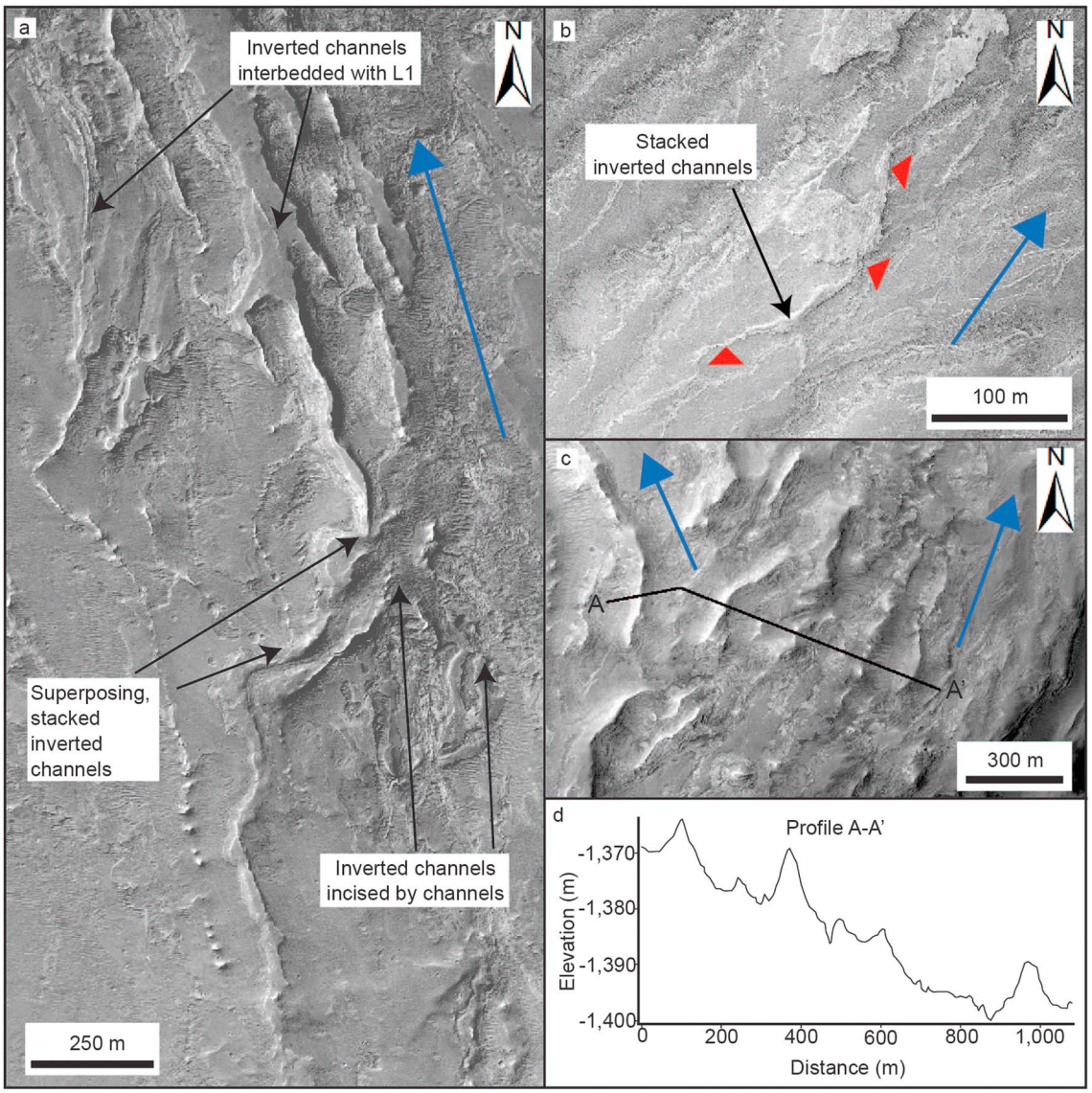

Figure 4. Examples of inverted channels throughout the basin. (a) HiRISE image of inverted channels in the East 1 drainage basin that are interbedded with L1. The inverted channels appear stacked in places, suggesting that the fluvial systems aggraded, and have subsequently been incised by later channels. Blue arrows show the downslope direction. (b) HiRISE image of stacked inverted channels (blue arrowheads) in the West 2 drainage basin. (c) HiRISE image of branching inverted channels in West 4 drainage basin and (d) their topographic profile from a HiRISE DEM.

(Strahler, 1958); West 1 and 2 have stream orders of up to eight. The highest measured sinuosity for any individual contiguous valley or channel is 1.39. Multiple examples of crosscutting and superposing channels are observed throughout the drainage networks (Figures 3 and 4). The planform morphology of erosional valleys and channels throughout the basin is generally subdendritic to subparallel (Figures 3 and S6 and Table 1; Zernitz, 1932). Channel meanders, scroll bars, or other evidence for lateral channel migration were not observed, with the exception of one highly localized example of channel meanders in the West 1 drainage network, which had been previously recognized (Williams & Weitz, 2014; Figure S6a).

Branching and sinuous ridges were identified throughout the drainage networks (Figures 4 and S6). These ridges are typically 10–50 m wide and 5–50 m high and form 1- to 2-km-long segments. The ridges vary in tone, appearing both medium-toned and very bright in HiRISE (RED) images. The ridges conform to local topography and appear in association with erosional valleys and channels throughout the basin. The planform geometry of these ridges is strong evidence that they are depositional channel systems now

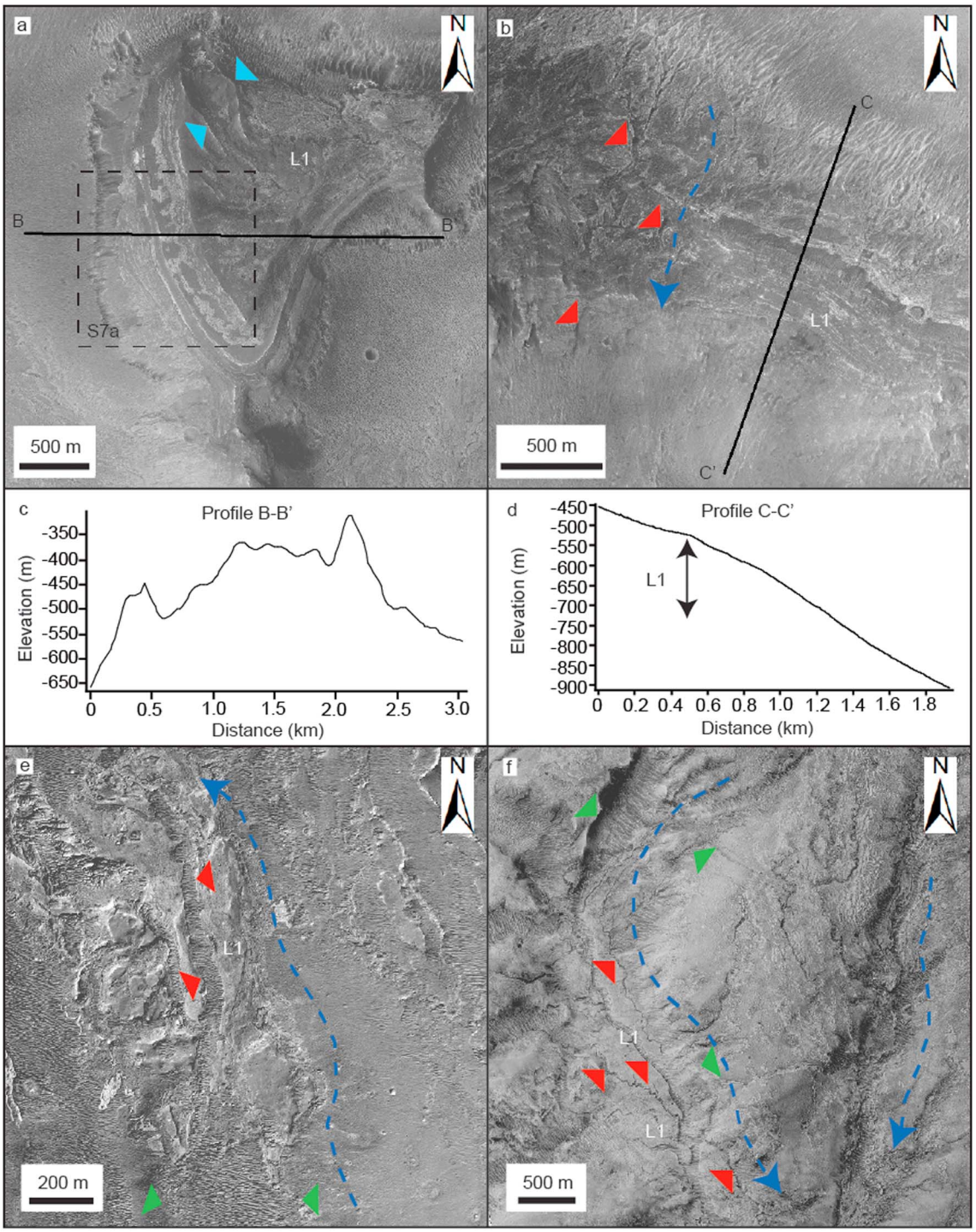

Figure 5. Examples of L1 throughout the basin. (a) HiRISE image of outlying sedimentary deposit of L1 ~ 350 m vertical thickness with inverted channels on its top surface (blue arrowheads); (b) HiRISE image of outlying sedimentary deposits of L1 ~ 200 m vertical thickness that are incised by channels. (c) Profile B-B′ of a from a CTX DEM showing that at least 350 m vertical thickness of L1 has been removed from the basin. (d) Profile C-C′ of (b) from a HiRISE DEM showing that at least 200 m vertical thickness has been removed from the basin. (e and f) HiRISE images of L1 infilling erosive fluvial valleys (green arrowheads) that has later been incised by channels (red arrowheads). Blue arrows show the downslope direction.

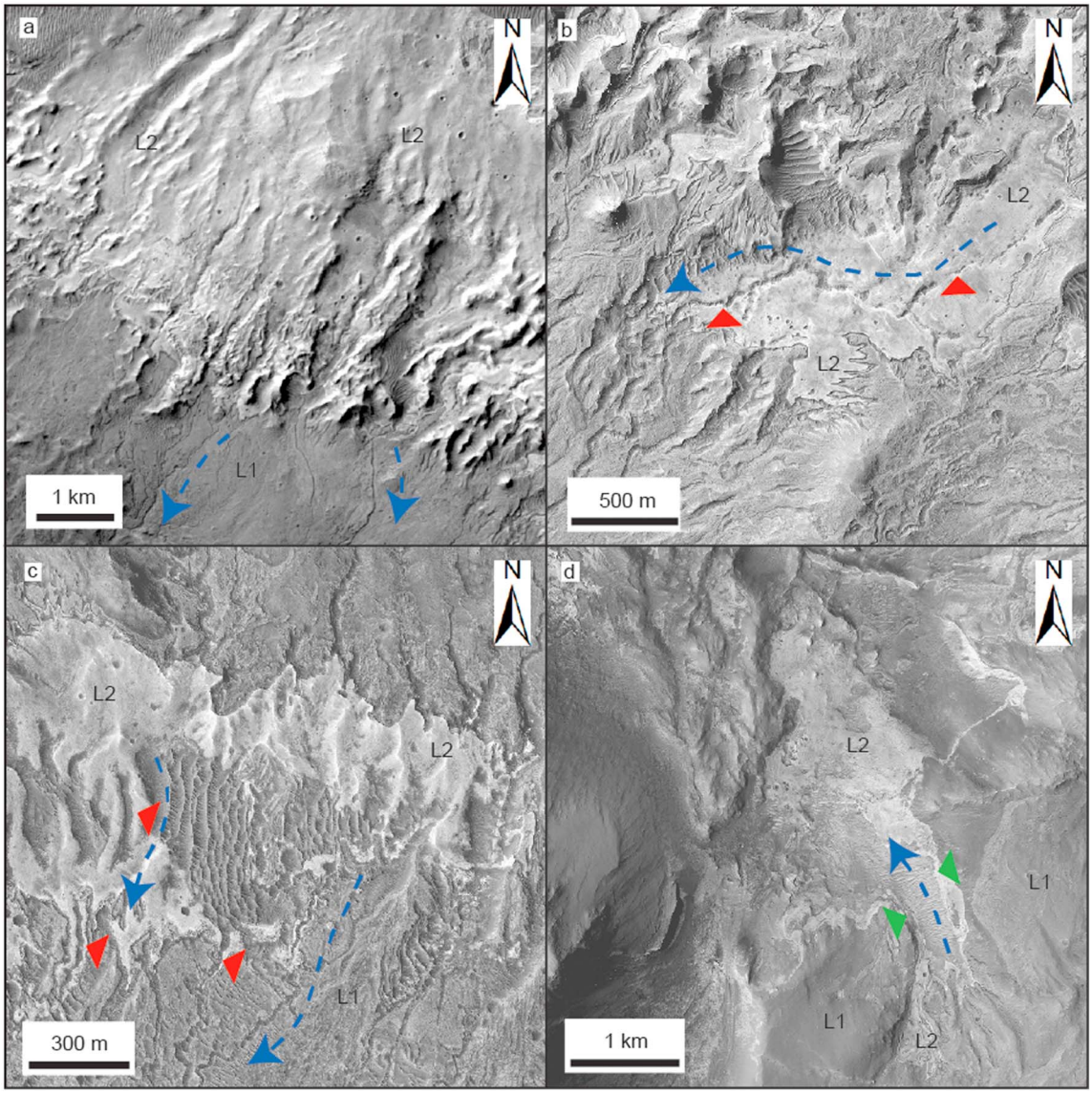

Figure 6. Examples of L2 throughout the basin. (a) CTX image of a bright, layered material (L2) found draping topography in the upslope areas of the basin. (b and c) HiRISE images of L2 that has been incised by fluvial channels (red arrowheads). (d) HiRISE image of L2 that has deposited in a fluvial valley (green arrowheads), which has not been incised by later channels. Blue arrows show the downslope direction.

preserved as inverted relief (inverted fluvial channels; Burr et al., 2010; Davis et al., 2016; Pain et al., 2007; Williams et al., 2009). These ridges are interpreted as inverted fluvial channels rather than glacial eskers as they conform to regional topography (i.e., they do not go upslope) and lack associated glacier landforms commonly found with eskers (e.g., Butcher et al., 2017; Gallagher & Balme, 2015). Alternatively, the ridges may be the eroded remnants of erosional valley walls; however, given that multiple tributary ridges converge in the downslope direction, they are more consistent with inverted channels.

These previously unrecognized inverted channels were found in five of the six drainage networks (absent in West 3; Table S3) and displayed a complicated stratigraphy. Multiple inverted channels are vertically stacked (Figure 4), indicating the aggradation of sediment in the basin. Many inverted channels are interbedded with or overprinted and incised by negative relief channels (Figures 4 and S6). Similar systems of superposing channels are observed in the negative relief fluvial systems elsewhere in the SMB (Figure S6). Thus, the catchment in the SMB contains both erosional valley networks and channel systems exposed in geomorphic relief, and exhumed depositional channel systems (inverted channels).

4.3. Relationship of Layered Deposits and Fluvial Systems in the Catchment

In this section, we describe how the fluvial systems relate to layered deposits found in the catchment of the basin. The erosional valley and channel networks in the basin catchment generally do not incise directly into the stacked lava flows thought to comprise the Valles Marineris walls (e.g., McEwen et al., 1999). As has been previously reported (Le Deit et al., 2010; Weitz et al., 2015; Williams & Weitz, 2014), erosional valleys and channels instead are incised into a generally medium-toned, draping material, which exhibits layering on the meter to decameter scale (herein referred to as L1; Figures 6, S7, and S8), strong evidence that it is sedimentary in origin. Although L1 is generally medium toned, it contains both darker and lighter layers (Figure S7a). The lighter toned layers frequently contain meter- to decameter-scale polygonal fractures and ridges on their surfaces (Figure S7b). L1 is pervasive throughout the SMB and is also observed to be interbedded with and overlying the fluvial systems (Figures 4, 5, S6, and S8). This is particularly noticeable in the East 1 drainage network, where L1 is interbedded between vertical stacked inverted channels (Figure 4). Prominent erosional outliers of L1 are found in the East 1 and 2 drainage networks, at least ~200–350 m in vertical thickness, into which erosional valleys and channels have incised and inverted channels are interbedded with (Figures 5a–5d). Broad erosional valleys have been infilled with L1, which has in turn been incised by subsequent channels (Figures 5e and 5f).

Stratigraphically above L1 is a light-toned, draping material, L2, which also exhibits layering on the meter to decameter scale (herein referred to as L2; Figure 6). L2 is best preserved in the upper reaches of the West 1 and 2 drainage networks (Figure 6a) but appears at multiple other locations throughout the SMB, where it has infilled many of the erosional valleys and channels (Figures 6b–6d). Only a few outcrops of L2 are present in the East 1 and East 2 drainage networks. As erosional valleys incise L1, L2 unconformably overlies L1. In some locations, L2 appears to have been incised or partially incised by narrow (10–20 m width; Figures 6b and 6c) channels, indicating that fluvial processes were active around the time that L2 was forming. The dissection of L2 (in four of the six drainage networks) is more geographically restricted than that of L1, and large-scale (hundreds of meters wide) erosional valleys, like those dissecting L1, do not dissect L2. The geographic distribution of these units is shown in Figure S8.

4.4. Relationship of the Catchment Landforms to Their Terminal Deposits

Here we examine the relationship of the fluvial landforms in the catchment to their terminal deposits in the paleolake system and at the other outlets for the basin, which lead into Valles Marineris. Note that we do not describe the geomorphology of the sediment fans in detail and mostly refer to the individual sediment fan descriptions/interpretations of Williams and Weitz (2014). Instead, we build on previous work by focusing on the stratigraphic relationship of the fans to the catchment, in particular whether the fans are sourced by the erosive or exhumed fluvial systems in the catchment described above.

The West 1 and East 1 networks drain into the paleolake from its western and eastern edges, respectively; but none of these fluvial systems appear to be an outlet for the paleolake (Figure 3). The fluvial systems in the catchment can be traced to elevations as low as ~−1,650 m in the paleolake, similar in elevation to the uppermost sedimentary fans interpreted as deltaic (Williams & Weitz, 2014). Three fan bodies (which we have labeled Fans 1, 2, and 3; Figures 7 and 8) are contiguous with the fluvial systems from West 1 and East 2 and superpose older lacustrine and deltaic deposits (Figure 7). These fans are arcuate shaped, have channels preserved on their top surfaces, and do not appear to have been exhumed. Underlying Fans 1–3 in the central paleolake are older fans, which generally comprise inverted channel and lobate deposits and are mostly interpreted as deltaic (Williams & Weitz, 2014; see Figures S1 and S2).

A key observation is that the catchment fluvial systems in the modern surface expression (e.g., erosional valleys and channels) do not appear to have directly fed sediment to these older fans (Figures 7 and 8). The former connection between West 1/East 1 and the older fan deposits within the SMB has been obscured by subsequent erosion. Thus, stratigraphic relationships suggest that most of the sedimentary fans in the paleolake were exhumed prior to the formation of the erosional valley and channels that are presently exposed in the SMB catchment. Fans of different ages are shown in Figure 7. Significant vertical thicknesses of lacustrine deposits in the paleolake (~400 m) appear to have been removed prior to the emplacement of Fans 1–3 (Figure 8e). The inverted relief associated with some sedimentary fans (Figures S1 and S2), and the indurated eolian bedforms in the paleolake (Figure S3; Williams & Weitz, 2014) are further evidence for exhumation.

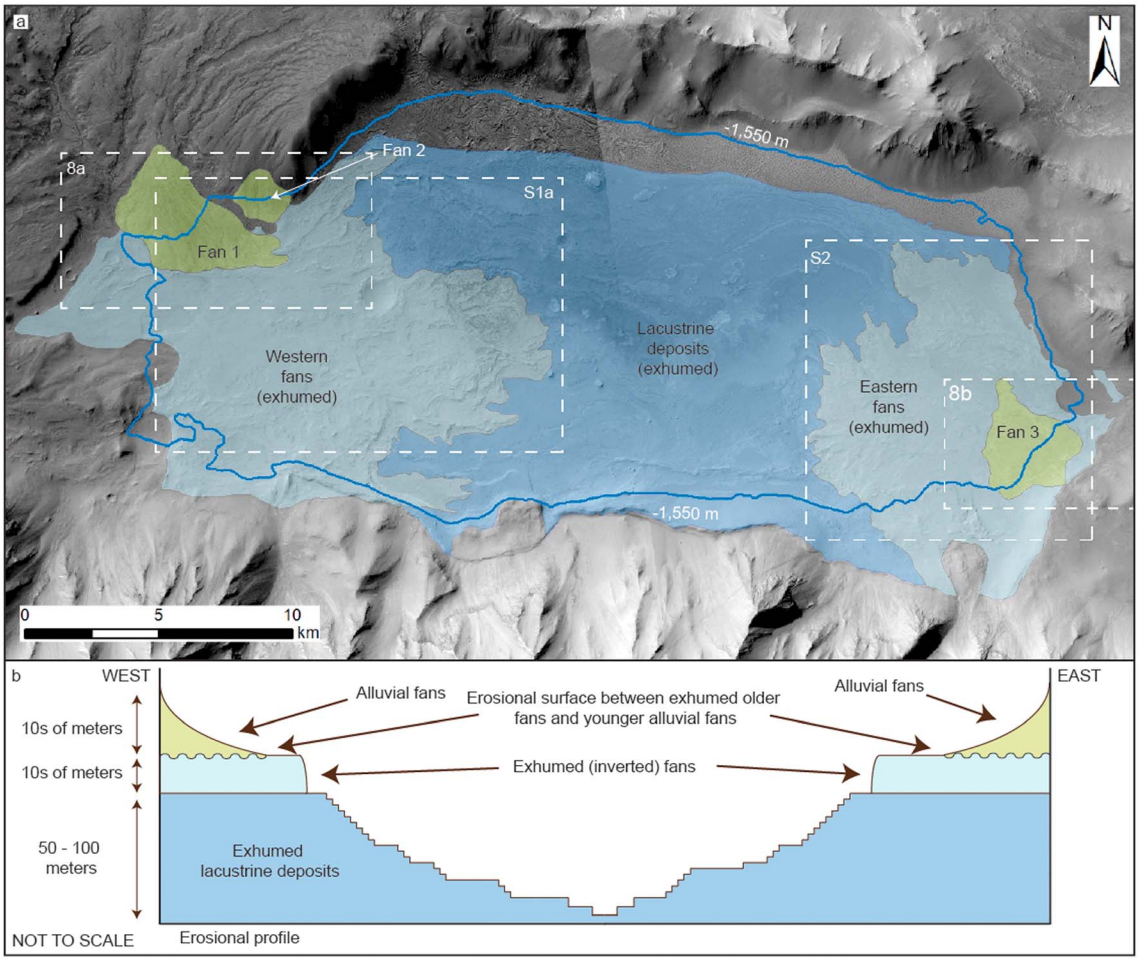

Figure 7. (a) CTX mosaic showing the older, exhumed deltaic and lacustrine deposits (blues), which are superposed by younger fans (green; Fans 1–3). (b) Simple cartoon cross section showing the relationships of different deposits in the paleolake. The western and eastern fans (see Figures 2, S1, and S2) mostly comprise inverted channel and lobate deposits and are generally interpreted as deltaic (see Williams & Weitz, 2014; Table S5). These fans do not appear to have been fed by the fluvial systems in West 1 or East 2 that are exposed in the present topographic expression. To contrast, Fans 1–3 are arcuate and have channels preserved on their surfaces, and appear to be directly fed from the erosional valleys and channels presently exposed in West 1 and East 1. This suggests that there was a period of erosion that exhumed the older fans in the paleolake, prior to the later emplacement of Fans 1–3.

Away from the paleolake, West 2–4 and East 2 appear to drain directly or indirectly into the main Melas Chasma trough (Figure 3). The fluvial systems within West 2 converge on a topographic depression at the northern edge of the basin (Figure 3c), which may form the site of a second smaller paleolake. There is a possible outlet in Melas Chasma at the northern end of the depression. Water would have to pass through this depression in order to reach the main Melas Chasma trough. For this to occur, the water level must have been at least 250 m high. The depression has since been infilled with material which postdates fluvial processes in the basin and as such no deposits (e.g., sedimentary fans) were identified, which would help confirm its origin as a paleolake.

4.5. Fluvial Landforms on the Valles Marineris Plateau

On the Valles Marineris plateaus, branching, erosional valley networks (hundreds of meters wide and tens of kilometers long; ~5–40 m deep) were identified converging on the headwalls of several tributary canyons at the western edge of Melas Chasma and along Ius Chasma (Figure 9). These branching valley networks are generally poorly preserved, which may be due to the low relief of the plateaus limiting the topographic expression of the valley networks, which can thus can be easily eroded and infilled. Although our mapping of these features only partially extended along Ius Chasma (~500 km), they were

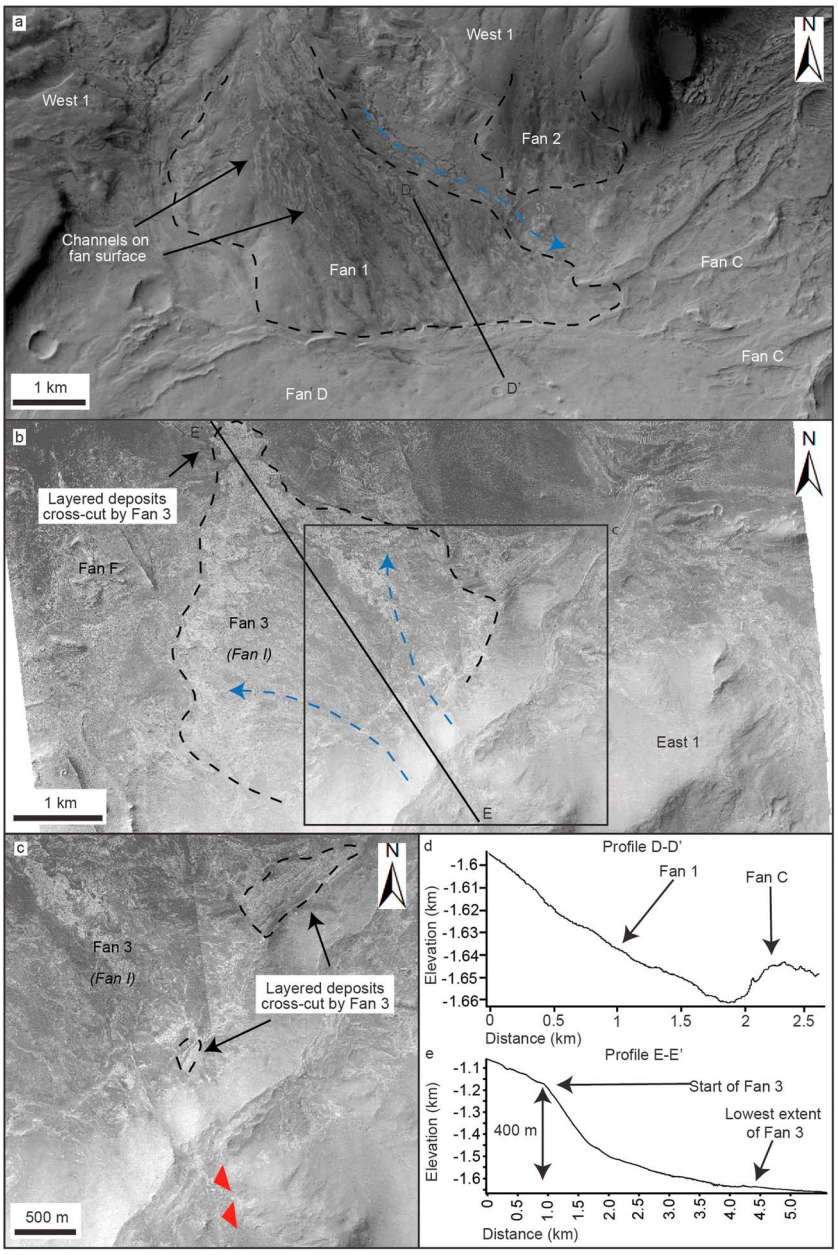

Figure 8. Sedimentary fans at the edges of the central paleolake. (a) CTX image of fans at the western boundary of the central paleolake. Channels from the West 1 drainage network are found on the top surfaces of Fans 1 and 2, but not on Fan C (Williams & Weitz, 2014). (b) HiRISE mosaic of Fan 3 at the eastern boundary of the central paleolake. (c) HiRISE mosaic of Fan 3, sourced by channels from the East 1 drainage network, and which crosscuts layered deposits in the paleolake. (d) Profile D-D′ (from a HiRISE DEM) showing the contact between Fan 1 and Fan C. The step in topography suggests that Fan C has been exhumed prior to the formation of Fan 1 and that Fans 1 and 2 are late-stage fans. (e) Profile E-E′ (from a HiRISE DEM) of Fan 3 at the eastern edge of the paleolake, which drapes over and crosscuts ~400 m vertical thickness of layered deposits, suggesting that these deposits were exhumed and eroded, prior to the formation of Fan 3.

found at most of the heads of the tributary canyons examined. The plateau valley networks are best preserved at the eastern end of the Ius Chasma plateau, although some valley networks do converge on canyon heads, which lead into the SMB (Figure 9). The contents within the tributary canyons themselves are mostly obscured by talus materials (Figure 9c). Many impact craters on the Melas and Ius plateau found in association with these erosional valley networks have degraded rims and little to

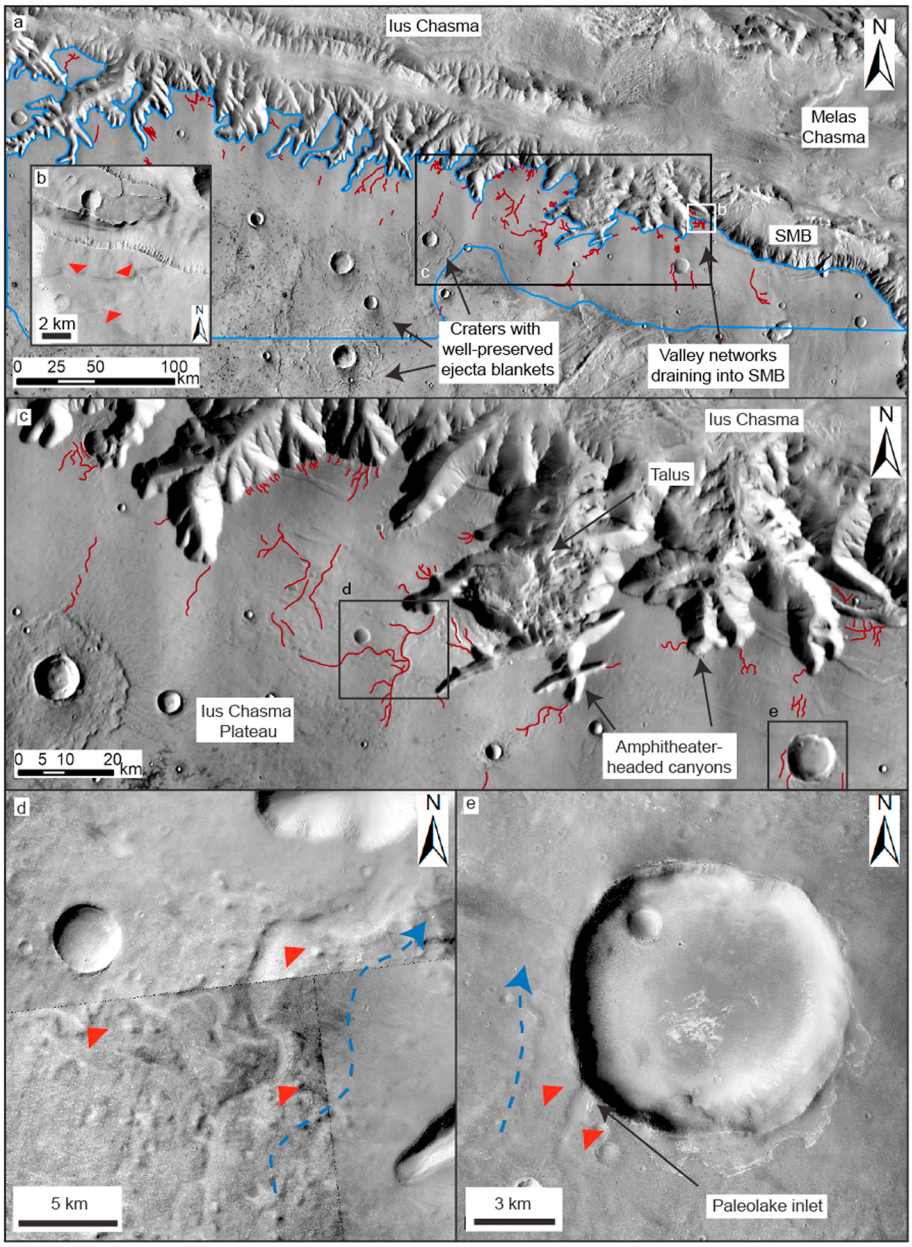

Figure 9. (a) Map of fluvial landforms (red lines) on the southern plateaus of Melas Chasma and Ius Chasma on a THEMIS-IR basemap; (b) CTX image of valley network (red arrowhead) converging on canyons, which lead into the southwest Melas basin; (c) map showing concentration of fluvial landforms (red lines) on the southern plateaus of Melas Chasma and Ius Chasma on a THEMIS-IR basemap; (d) CTX mosaic of branching valleys networks (red arrows) converging on the heads of tributary canyons on the southern walls of Ius Chasma; and (e) CTX image of valley networks breaching the rim of an impact crater (forming a paleolake).

no impact ejecta (Figure 9e), consistent with having been eroded (e.g., Craddock et al., 1997; Craddock & Howard, 2002). Furthermore, erosional valley networks have breached into several of these impact craters, indicating that water may have ponded, potentially forming small paleolakes (Figure 9e). To contrast, superposing the plateau valley networks, there are large impact craters with well-preserved rims and ejecta blankets that have not been significantly eroded (Figure 9a). This suggests that crater degradation may have mostly been due to fluvial erosion.

5. Discussion

5.1. Formation of the Catchment Fluvial Systems

Our mapping of fluvial landforms indicates that fluvial activity was widespread over the entire SMB and on the adjacent Valles Marineris plateaus (Figures 3 and 9). The fluvial systems in the SMB catchment have high stream orders (4–8) and drainage densities (0.22–1.97 km^{-1}); the West 3 and 4 and the East 1 and 2 drainage networks are significantly more mature than previously reported (Quantin et al., 2005; Williams & Weitz, 2014). Very few of the drainage networks form single thread channel systems or solitary valleys; high-resolution images of these areas demonstrate significantly greater concentrations of fluvial systems than previously identified using lower-resolution data (Mangold et al., 2004; Quantin et al., 2005). There is also evidence from the topography of West 2 drainage network that other paleolakes existed within the basin, in addition to the main paleolake system (Figure 3c).

Drainage density values (Tables 1 and S4) are among some of the highest reported values for martian valley and channel networks (Hynek et al., 2010). Even the lowest value (0.22 km^{-1} for West 3) is well above the mean values for Noachian valley networks (0.0115 km^{-1}; Hynek et al., 2010), which are indicative of long-lived sediment routing systems that were continuously active or frequently recharged. The highest drainage density values (>1 km^{-1}) are within the range of values for terrestrial systems (Carr & Chuang, 1997) and similar to at least one drainage system observed elsewhere in Valles Marineris (e.g., plateau above Juventae Chasma; 0.9–2.3 km^{-1}; Williams et al., 2005). These high values, along with other fluvial characteristics, are consistent with all the fluvial systems in the SMB being formed by precipitation-driven (either rainfall or snowfall) surface runoff (e.g., Craddock & Howard, 2002; Hynek et al., 2010; Hynek & Phillips, 2003). Water may have been sourced from both inside and outside the SMB.

5.2. Evolution of Fluvial Processes in the SMB

The stratigraphy of the fluvial systems in the SMB is complex but consistent with recurrent fluvial processes. We summarize the proposed sequence of development in Figure 10 and discuss the observational evidence supporting various phases in the following text. The stratigraphic context of the fluvially dissected unit L1, presumably an ash or atmospheric dust unit (Weitz et al., 2015), indicates that it was emplaced over a prolonged period. The erosional outliers of L1 indicate that significant amounts of material were removed from the drainage basins, at least ~200–350 m vertical thickness, as indicated by their minimum thicknesses (Figure 5). The emplacement and erosion timing of L1 can be explained by several scenarios: (1) L1 is unrelated to the fluvial systems and was mostly eroded prior to the onset of fluvial processes, perhaps by eolian abrasion, (2) L1 formed prior to the onset of fluvial processes but was primarily eroded by fluvial processes, which would be consistent with the large volumes of fluvially transported material in the paleolake, or (3) L1 was forming contemporaneously with fluvial processes and being episodically removed by fluvial erosion. Given that L1 can be traced throughout the basin and that it drapes rather than infills topography, L1 is unlikely to be entirely fluvial sediment. However, the interbedded stratigraphy of L1 and the fluvial systems (Figures 4 and 5) suggests fluvial processes were probably involved in at least some of the modification of L1 while it was forming.

The color and brightness variations suggest that there are compositional or textural variations between layers within L1 (Figures 4, 5, and S7). For example, the darker-toned layers could be unaltered ash, dust, or eolian materials, whereas the lighter-toned layers could have been mineralogically altered through interaction with water, inferred for layered deposits elsewhere on the Valles Marineris plateaus (Weitz et al., 2008, 2010). Polygonal fractures and ridges, such as those that are present in the lighter-toned L1 layers, have been associated with desiccation elsewhere on Mars (e.g., El-Maarry et al., 2014), in addition to numerous other formation mechanisms, such as burial and reexposure, thermal contraction, or fluid deposition of resistant minerals in fractures (e.g., Brooker et al., 2018; Levy et al., 2010). Ash, dust, and eolian material could have accumulated throughout the basin, only to be contemporaneously altered and removed by fluvial processes. A problem with much of L1 being mineralogically altered through interaction within water is that the basin generally lacks hydrated mineral signatures (Weitz et al., 2015). However, this could be due to a low water-rock ratio limiting the amount of aqueous alteration (e.g., Rice et al., 2017) or simply because of an absence of detection, possibly the result of dust cover or insufficient resolution (e.g., Murchie et al., 2009).

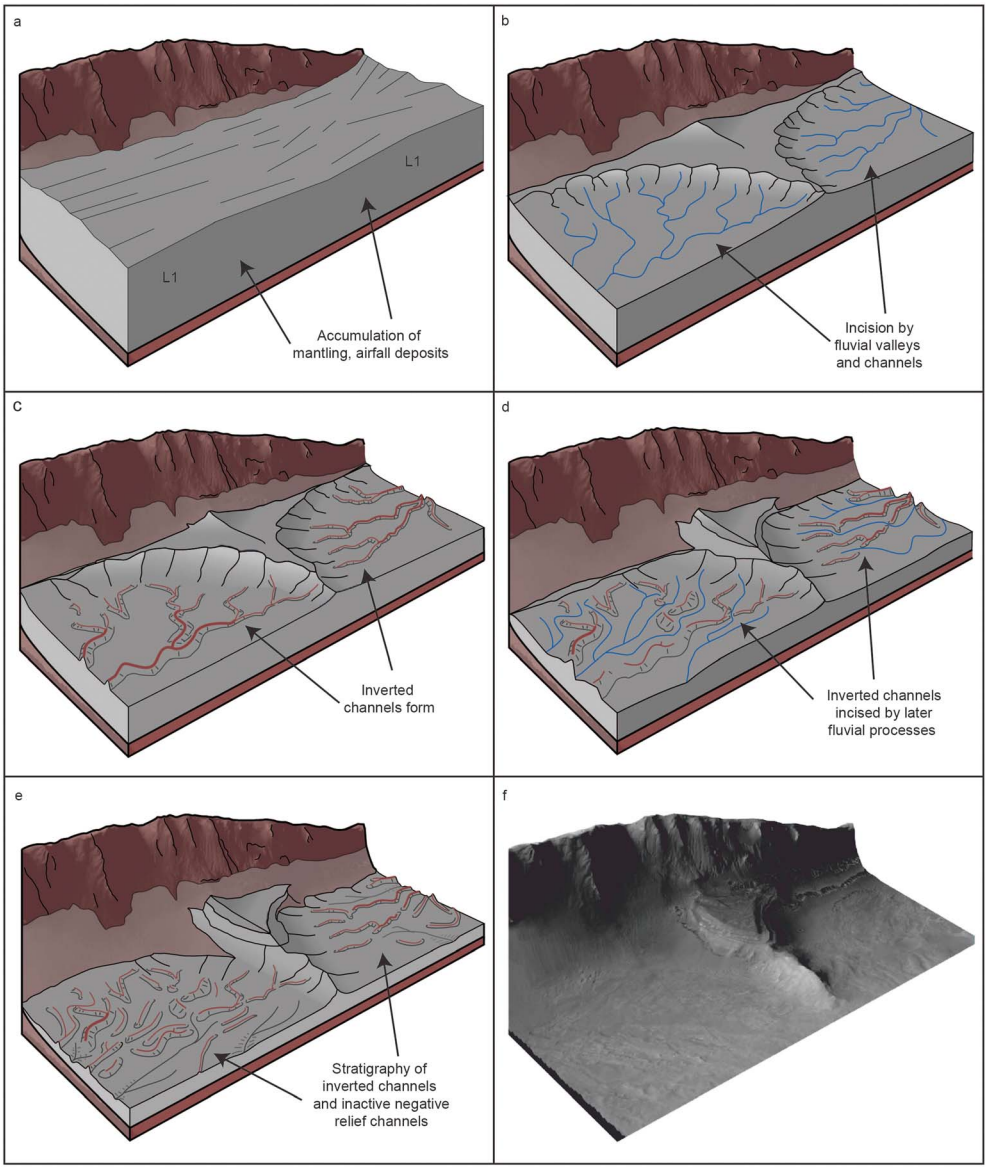

Figure 10. Simplified schematic showing the evolution of the East 1 and 2 drainage networks. (a) Airfall material (L1) accumulates on the canyon basement material, interspersed with multiple periods of fluvial activity (blue lines) and erosion (b–d). This leads to the development of inverted channels (red lines) and a pronounced East 1 to East 2 watershed (c). The inverted channels have themselves been incised by later channels (d). Today, the drainage networks comprise a mixture of inverted and negative relief channels (e). (f) Perspective (facing northeast) CTX DEM of the East 1 and 2 drainage networks. Note that L2 is generally not found in the East 1 and 2 drainage networks and therefore not been included in the schematic. The emplacement of L2 postdates the events shown in panels a–c.

The existence of inverted channels in several of the drainage basins indicates that fluvial channel deposits were cemented, buried, and later exhumed, probably be eolian abrasion (Burr et al., 2010; Pain et al., 2007; Williams et al., 2009). The inverted channels likely comprise at least some fluvial channel sediment; however, they could also comprise L1 material that infilled channels. The channel bodies may have become cemented by circulating groundwater (e.g., Pain et al., 2007), which may have also partly cemented L1. Either during the cementation, burial, or exhumation of the channels, fluvial processes in the basin, at least locally, probably waned or ceased entirely, leading to a dry phase when the inverted channels formed (e.g., Pain et al., 2007). Deposits of L1 may have had time to accumulate without being eroded away if fluvial processes ceased (e.g., as are now preserved in the wide erosional valleys; Figures 5 and S6). Yet the inverted channels and the L1 deposits within valleys have themselves been incised by fluvial channels (Figures 4, 5, and S6),

indicating that fluvial processes in the basin later resumed. Multiple stacks of inverted channels at different stratigraphic levels that have been incised by later channels indicate that this "wet-dry" sequence repeated several times (Figures 4 and 10). Further indurated and lithified channel bodies may be buried within L1. Thus, throughout much of the history of the basin, fluvial processes were most likely episodic.

While the formation and erosion of L1 by the fluvial systems is difficult to temporally constrain, it does not appear to have been a sudden event; hundreds of meters of material were deposited and eroded. Assuming a range of different denudation rates from analogue environments on Earth (10^{-3} to 10^{-4} m/year; Saunders & Young, 1983), the erosion of 200–350 m of L1 would have taken ~10^5–10^6 years, suggesting that fluvial processes in the SMB may have lasted at least this long (see Table S6 for details). The development of stacked, aggrading channels (e.g., Figure 4) locally within erosional valleys in the catchment may be due to the high sediment flux from the erosion of L1. In terrestrial channel systems, aggradational environments can develop in regions of slow subsidence, where the landscape cannot remove the influx of sediment fast enough, or in regions with large amounts of available accommodation space or a rising base level (e.g., Smith, 1983, 1986). The presence of aggrading channels systems in the SMB suggests that the basin may have fully formed by the time the fluvial systems were active or at least the rate of subsidence was so low that it could not accommodate the erosion of L1. Alternatively, the aggrading channel systems could be due to a rising base level, possibly driven by rising water depths in the paleolake, leading to localized channel backfilling in the catchment.

Overlying L1, unit L2 has also infilled the erosional valley and channel networks through the basin (Figure 6), indicating that fluvial processes were waning considerably or had ceased entirely when L2 was forming. However, as L2 itself has been dissected by channels (Figure 6), fluvial processes were active after the formation of L2. The presence of hydrated silica and sulfates within L2 (Weitz et al., 2015) is further evidence for aqueous alteration. L2 appears to have been reworked from upslope regions higher up in the basin (Weitz et al., 2015). Mass wasting could have reworked the L2 deposits from upslope into the dry fluvial valleys, only for the deposits to be dissected by a later, waning fluvial phase. Alternatively, fluvial processes could have reworked the L2 deposits downstream into the valleys; however, this is difficult to reconcile with the majority of L2 deposits that are not dissected by channels (Figure 6d). Unlike L1, wide erosional valleys do not dissect L2. Taking channel width as a proxy for discharge (e.g., Irwin, Craddock, et al., 2005; Williams et al., 2009), the narrow width of the channels dissecting L2 and their geographically limited extent indicates that by this point, conditions in the basin were becoming increasingly ephemeral.

Similar trends indicative of episodic fluvial processes are observed in the paleolake. Midway up the lacustrine succession, the field of indurated eolian bedforms identified by Williams and Weitz (2014) indicates a period of subaerial exposure, possibly during a lowstand in the lake or when it was dry entirely (Figure S3). The cementation of these features may have occurred due to circulating groundwaters or diagenetic fluids. As this surface is overlain by further packages of lacustrine deposits and sedimentary fans, the lake refilled subsequently (Williams & Weitz, 2014). Further periods of subaerial exposure in the paleolake are found near the top of the lacustrine succession. At the western end of the paleolake, Fan C (after Williams & Weitz, 2014) is preserved in inverted relief, and it is unconformably overlain by Fan 1 (Figure 8a). Many other fans near the top of the lacustrine succession are also preserved in inverted relief (Figures S1 and S2). Similarly, at the eastern end of the paleolake, Fan 3 unconformably drapes over the lacustrine deposits, where at least ~400 m vertical thickness has been removed (Figure 8). These unconformable contacts indicate a possible hiatus in fluvial and lacustrine activity, during which the erosion of the lacustrine deposits and the exhumation of the fans occurred. This thickness of material removed in the paleolake is comparable to the thickness of L1 removed from the catchment (~200–350 m; Figure 5).

However, as both the lacustrine deposits and fans are overlain by subsequent fans (Fans 1–3; Figures 7 and 8), fluvial processes likely resumed in the later history of the paleolake. Fans 1–3 have channels on their surfaces and are clearly sourced from the uppermost fluvial systems in the drainage networks, unlike the other fans in the paleolake, which are preserved in inverted relief. This indicates that Fans 1–3 are most likely late-stage fans. Whether the paleolake contained water at the time of Fans 1–3 is difficult to determine. Although distinguishing between alluvial and deltaic fan systems is difficult from remote sensing data alone, none of these Fans 1–3 have strong geomorphic evidence that would support a deltaic origin (e.g., Van Dijk et al., 2009, 2012). Unlike many of the older fans, Fans 1–3 are found near the edge of the paleolake and are not

clearly interfingered with the lacustrine deposits. These characteristics suggest that Fans 1–3 are alluvial fans and that by this point in the basin's evolution, the level of water in the paleolake was low or it was entirely dry. The geomorphology and stratigraphy of both the fluvial systems in the catchment and of the paleolake thus indicate that liquid water went from being episodically and widely available throughout the basin, to being sparsely available and geographically restricted. Previous estimates of formation timescales for individual sediment fans and the lacustrine deposits range from 10^2 to 10^5 years (Metz et al., 2009; Williams & Weitz, 2014). These estimates are lower than our erosion period of L1, which also constrains the duration of fluvial processes (10^5–10^6 years; Table S6). However, given the numerous hiatuses and unconformities observed in both the catchment and the paleolake, we suggest that aqueous processes may have lasted for significantly longer than this.

5.3. Regional Fluvial Processes

Fluvial activity does not appear to have been constrained to the SMB. On the plateaus above Melas and Ius Chasma, the presence of wide, branching valley networks (Figure 9), which drain into the amphitheater-headed tributary canyons on the southern wall of Ius Chasma, suggests that precipitation and surface runoff was involved in canyon formation and modification (e.g., Lamb et al., 2006, 2008). Amphitheater-headed canyons on Mars (including those leading into Ius Chasma) have been associated with groundwater seepage erosion (e.g., Goldspiel, 2000; Laity & Malin, 1985; Lucchitta et al., 1992). However, the presence of branching erosional valleys at the heads of these canyons, which originate at multiple elevations, is inconsistent with forming solely due to groundwater seepage. Instead, the formation of these valleys likely required precipitation-driven runoff, which originated across a wide area (e.g., Craddock & Howard, 2002; Hynek et al., 2010; Hynek & Phillips, 2003).

The formation of amphitheater-headed canyons is controversial. Terrestrial studies of the closest analogues for amphitheater-headed canyons, which incise into consolidated rock (e.g., Box Canyon in Idaho; Lamb et al., 2006, 2008) have found that groundwater seepage plays a secondary role to runoff and that high magnitude flash floods are probably needed for eroding and transporting large volumes of material, although seepage may play a role in producing the rounded shape of the canyon heads (Pelletier & Baker, 2011). The walls of Melas and Ius Chasma appear to be composed of consolidated rock (i.e., stacked lava flows; e.g., McEwen et al., 1999), which likely requires high discharge to become incised (Lamb et al., 2006; Lamb et al., 2008). The presence of branching valleys at the canyon heads would be consistent with flash floods, and the occurrence of flash floods would make it difficult to exclude the occurrence of more perennial episodes of runoff on the plateaus. Water may have ponded in the degraded and eroded craters on the plateau forming paleolakes (Figure 9e).

We emphasize, however, that this does not exclude the role of groundwater seepage, which is predicted to have been emerging regionally from the canyon walls due to a near surface water table (e.g., Andrews-Hanna et al., 2010), and draining into Valles Marineris. This combined role is supported by recent topographic and morphometric analyses of the Ius Chasma tributary canyons themselves (Martha et al., 2017), and the presence of poorly preserved valley networks that are connected to amphitheater-headed canyons elsewhere around Valles Marineris (Mangold et al., 2008), indicating that runoff, in addition to groundwater seepage, occurred more regionally and was involved in canyon modification.

Some of the fluvial systems drain into canyons, which lead into the SMB (Figure 9b), suggesting that some water in the SMB was supplied by runoff from the plateau. Emerging regional groundwater at the canyon walls was also likely draining into the SMB (e.g., Andrews-Hanna et al., 2010). However, constraining whether fluvial processes on the plateau were active contemporaneously with fluvial processes in the SMB is challenging. On the global map of Tanaka et al. (2014), the fluvial systems on the Melas and Ius plateau incise into an early Hesperian volcanic unit (Tanaka et al., 2014). Upon inspection with high-resolution data, these terrains actually comprise layered sedimentary material, also considered Hesperian in age and which overlies the volcanic units (Le Deit et al., 2010; Weitz et al., 2008, 2010).

The units within the SMB are considered early Hesperian (Quantin et al., 2005), although we recognize that a Hesperian age derived from crater statistics alone should be treated with caution due to the artificial exclusion of large craters across a small count area (e.g., Warner et al., 2015) and the extensive modification of the landscape by erosion. However, as western Valles Marineris is thought to have formed during the late

Noachian to early Hesperian (e.g., Anderson et al., 2001; Andrews-Hanna, 2012; Schultz, 1991; Witbeck et al., 1991) and the SMB deposits overlie the Valles Marineris wall rock (and postdate canyon formation), a Hesperian age would be broadly consistent with that stratigraphy (although an older Noachian age cannot be entirely excluded). Hesperian precipitation and runoff on the plateau might therefore have occurred contemporaneously with similar processes in the basin; however, given that fluvial processes in the basin were likely episodic, it cannot be determined definitively.

5.4. Proposed Geological History of the SMB and Plateau

The lowermost exposed sedimentary material in the basin is L1, which is probably composed of eolian, dust, or ash deposits. The onset of L1 deposition was followed by fluvial activity, primarily driven by precipitation, but perhaps also supported by regional groundwater emerging at the canyon wall and runoff from the plateau draining into the SMB, beginning the formation of the valley networks. Fluvial processes were active on the plateaus south and west of the SMB and likely contributed to the widening of the tributary canyons on the southern wall of Ius Chasma.

Repeated "wet and dry" phases in the SMB led to episodic accumulation and erosion of L1. During the wet phases, fluvial incision, erosion, and possibly the mineralogical alteration of L1 occurred. The bright-toned layers within L1 may represent materials that were altered during fluvial phases. Eroded material was transported downstream to the paleolake, forming sedimentary fans and lacustrine deposits (Williams & Weitz, 2014), and into Melas Chasma. Additional, smaller paleolakes elsewhere in the basin may have existed during this time. During the dry phases, L1 continued to accumulate, but was not altered by aqueous activity, and began to fill erosional valleys. During the dry phases depositional channels in the catchment were exhumed and inverted due to differential erosion. Cumulatively throughout the wet and dry phases, several hundred meters of material were eroded from the catchment and the paleolake. Near the end of the L1 emplacement, or soon after, Fans 1–3 were formed in the central paleolake, possibly as alluvial fans.

At some point after L1 deposition ended, the magnitude of fluvial activity waned or paused. L2 then began to form, likely also as airfall deposits. L2 was aqueously altered (Weitz et al., 2015) and transported down slope, possibly by fluvial processes. The magnitude of the fluvial activity, while still relatively widespread, appears to have been significantly reduced during this time, as indicated by the partially filled erosional valleys. Fluvial processes were probably not active in the West 3 and 4 drainage networks during this period. This reduction in fluvial processes could be due to transitions from a perennial to an ephemeral setting, in conjunction with a drying climate. The total period for aqueous processes may be $>10^5$ years. Sometime after this, fluvial activity ceased entirely and the valley networks were subsequently modified by eolian and mass wasting processes alone.

5.5. Implications for Regional Valles Marineris Climate and Environment

The geological evidence from the SMB and the surrounding plateaus indicates that this region of Valles Marineris was extensively modified by long-lived and episodic aqueous processes in the Hesperian, with water probably supplied by a combination of precipitation (e.g., Craddock & Howard, 2002; Hynek et al., 2010; Hynek & Phillips, 2003), emerging groundwater from the canyon walls (e.g., Andrews-Hanna et al., 2010), and runoff from the plateau. However, the question remains: Why was there precipitation and runoff here? Aqueous processes here most likely postdate the climate optimum at the end of Noachian (e.g., Fassett & Head III, 2008a; Irwin, Howard, et al., 2005). A changing climate in the Hesperian likely reduced the global availability of liquid water (e.g., Bibring et al., 2006). Thus, there could be significant local and regional factors around Valles Marineris causing precipitation and runoff (e.g., higher local pressures and temperatures within the depths of Valles Marineris, or perhaps elevated local geothermal heat; Kite et al., 2011).

Both the drainage networks and paleolake reveal vertical transitions in their stratigraphy, which may reflect the drying environment and changing climate. While there is strong evidence that aqueous processes were episodic in the SMB (e.g., the infilled and incised erosional valleys, the incised inverted channels, and the periods of subaerial exposure the paleolake), the decrease in aqueous processes became terminal in the later history of the basin. The youngest valleys and channels are geographically restricted, narrow, and are mostly single threaded. This is consistent with a decrease in the availability of surface water, as seen in arid, ephemeral environments on Earth. Similarly, within the central paleolake, the deposits transition from a

deltaic-lacustrine setting, to a possible alluvial one, with deposits concentrated around the edge of the paleolake, again indicating a terminal decrease in the availability of surface water.

Many of the fluvial features identified in the SMB are only recognizable at HiRISE resolution (0.25 m per pixel). Similarly, the fluvial features identified on the Valles Marineris plateaus are only recognizable at CTX resolution (6 m per pixel) or greater. This begs the question of whether Hesperian fluvial processes in the SMB region were a rare or special case within Valles Marineris, or whether the site is just exceptionally well preserved. Recently identified HiRISE- and CTX-scale fluvial features in Juventae Chasma (e.g., Singh et al., 2017; Weitz et al., 2008), Coprates Chasma (e.g., Grindrod et al., 2012, 2017), and on the Valles Marineris plateaus (e.g., Le Deit et al., 2010; Mangold et al., 2008; Weitz et al., 2008, 2010; Williams et al., 2005), suggest that fluvial systems may be common in Valles Marineris and that of these, the SMB is an exceptionally well-preserved example. A similar stratigraphy of multiple generations of channel networks is found in Juventae Chasma (Singh et al., 2017; Williams & Weitz, 2009), suggesting that fluvial processes were also episodic in the wider region. We would expect similar fluvial systems to be preserved elsewhere in the canyons of Valles Marineris and on its plateaus, and for those to be identified as more HiRISE coverage becomes available. This would indicate that fluvial processes were widespread across Valles Marineris during the Hesperian.

6. Conclusions

New high-resolution mapping of fluvial landforms in the SMB indicates the basin underwent long-lived, episodic, but ultimately waning fluvial processes. Fluvial systems in the basin catchment are preserved as erosional valleys and channels and inverted channels. These systems appear to have supported at least two paleolake systems within the basin (Quantin et al., 2005; Williams & Weitz, 2014). The fluvial morphologies are consistent with formation by widespread precipitation and runoff throughout the basin.

The existence of inverted channels in the catchment, themselves incised by later channels, indicates a pause in fluvial activity where depositional channels were exhumed. Similarly, erosional valley networks have both incised into and been filled by layered, sedimentary material, possibly while the fluvial systems were inactive. In some cases, this valley fill material has itself been incised by later channels. This draping, layered sedimentary material is pervasive throughout the catchment and is likely airfall material, which was being emplaced and eroded contemporaneously with fluvial processes. Erosional outliers of this sedimentary material are incised by and interbedded with fluvial landforms, indicating that large volumes of material were removed by erosion. These stratigraphic relationships indicate that the basin underwent repeated episodes of "wet and dry" phases, during which fluvial processes interchanged with deposition of airfall material and periods of eolian erosion. Many erosional valleys have been filled by late-stage sedimentary material, which is generally not incised by channels, suggesting that toward the later history of the basin, fluvial processes appear to have ultimately waned, before ceasing entirely.

At the edges of the central paleolake, the uppermost erosional fluvial systems in the catchment superpose the exhumed deltaic and lacustrine deposits in the paleolake, which is further evidence for at least one erosional horizon within the fluvial succession. The exhumation of the deltaic and lacustrine deposits occurred prior to the emplacement of several late-stage sediment fans, which may be alluvial fans. This is strong evidence for fluctuations in lake level while the fluvial systems were active, which is also supported by the presence indurated eolian bedforms in the paleolake succession (Williams & Weitz, 2014). The occurrence of multiple wet and dry phases in the catchment is thus reflected in the paleolake succession.

Recurrent aqueous processes in the SMB during the Hesperian postdates the climate optimum and global valley-forming phase inferred at the Noachian/Hesperian boundary (e.g., Fassett & Head III, 2008a; Irwin, Howard, et al., 2005). Local or regional factors may therefore have made conditions more favorable to liquid water here within a drying and cooling climate. Finally, fluvial systems are observed on the tops of the Melas and Ius Chasma plateaus, although are generally poorly preserved; some of these may have supplied the drainage networks in the SMB, and many appear to have drained into tributary canyons that lead into Ius Chasma. Thus, it is possible that the SMB fluvial systems are observed owing to exceptional preservation factors and that episodic fluvial activity occurred more widely throughout the Valles Marineris region.

Acknowledgments
J. M. D. gratefully acknowledges Science and Technology Facilities Council (STFC) and UK Space Agency (UK SA) funding (ST/K502388/1 and ST/R002355/1) and additional funding from the Royal Astronomical Society and the British Society for Geomorphology. P. M. G. acknowledges UK SA funding (ST/L00254X/1). P. F. was funded by UK SA grant ST/R001413/1. R. M. E. W. gratefully acknowledges funding from NASA's Mars Fundamental Research Program (NNX13AG83G). S. G. acknowledges UK SA funding (ST/L006413/1). M. B. was funded by UK SA grants ST/L00643X/1 and ST/R001413/1. We thank Frances Butcher for useful discussions. We thank the various Mars instrument teams for their consistent and dedicated work. The standard data products used here are available from the NASA PDS (https://pds.jpl.nasa.gov/). The HiRISE and CTX DEMs are available for download at https://doi.org/10.6084/m9.figshare.c.4119992. We thank two anonymous reviewers for their thorough and constructive comments.

References

Anderson, R. C., Dohm, J. M., Golombek, M. P., Haldemann, A. F. C., Franklin, B. J., Tanaka, K. L., et al. (2001). Primary centers and secondary concentrations of tectonic activity through time in the western hemisphere of Mars. *Journal of Geophysical Research*, *106*(E9), 20,563–20,585. https://doi.org/10.1029/2000JE001278

Andrews-Hanna, J. C. (2012). The formation of Valles Marineris: 3. Trough formation through super-isostasy, stress, sedimentation, and subsidence. *Journal of Geophysical Research*, *117*, E06002. https://doi.org/10.1029/2012JE004059

Andrews-Hanna, J. C., Zuber, M. T., Arvidson, R. E., & Wiseman, S. M. (2010). Early Mars hydrology: Meridiani playa deposits and the sedimentary record of Arabia Terra. *Journal of Geophysical Research*, *115*, E06002. https://doi.org/10.1029/2009JE003485

Balme, M., Berman, D. C., Bourke, M. C., & Zimbelman, J. R. (2008). Transverse Aeolian Ridges 617 (TARs) on Mars. *Geomorphology*, *101*(4), 703–720. https://doi.org/10.1016/j.geomorph.2008.03.011

Bibring, J.-P., Langevin, Y., Mustard, J. F., Poulet, F., Arvidson, R., Gendrin, A., et al. (2006). Global mineralogical and aqueous mars history derived from OMEGA/Mars Express data. *Science*, *312*(5772), 400–404. https://doi.org/10.1126/science.1122659

Brooker, L. M., Balme, M. R., Conway, S. J., Hagermann, A., Barrett, A. M., Collins, G. S., & Soare, R. J. (2018). Clastic polygonal networks around Lyot crater, Mars: Possible formation mechanisms from morphometric analysis. *Icarus*, *302*, 386–406. https://doi.org/10.1016/j.icarus.2017.11.022

Burr, D. M., Williams, R. M. E., Wendell, K. D., Chojnacki, M., & Emery, J. P. (2010). Inverted fluvial features in the Aeolis/Zephyria Plana region, Mars: Formation mechanism and initial paleodischarge estimates. *Journal of Geophysical Research*, *115*, E07011. https://doi.org/10.1029/2009JE003496

Butcher, F. E. G., Balme, M. R., Gallagher, C., Arnold, N. S., Conway, S. J., Hagermann, A., & Lewis, S. R. (2017). Recent basal melting of a mid-latitude glacier on Mars. *Journal of Geophysical Research: Planets*, *122*, 2445–2468. https://doi.org/10.1002/2017JE005434

Carr, M. H. (1995). The martian drainage system and the origin of valley networks and fretted channels. *Journal of Geophysical Research*, *100*(E4), 7479–7507. https://doi.org/10.1029/95JE00260

Carr, M. H., & Chuang, F. C. (1997). Martian drainage densities. *Journal of Geophysical Research*, *102*(E4), 9145–9152. https://doi.org/10.1029/97je00113

Chapman, M. G., & Tanaka, K. L. (2001). Interior trough deposits on Mars: Subice volcanoes? *Journal of Geophysical Research*, *106*(E5), 10,087–10,100. https://doi.org/10.1029/2000JE001303

Christensen, P. R., Jakosky, B. M., Kieffer, H. H., Malin, M. C., McSween, H. Y., Jr., Nealson, K., et al. (2004). The Thermal Emission Imaging System (THEMIS) for the Mars 2001 Odyssey Mission. *Space Science Reviews*, *110*, 85–130.

Craddock, R. A., & Howard, A. D. (2002). The case for rainfall on a warm, wet early Mars. *Journal of Geophysical Research*, *107*(E11), 5111. https://doi.org/10.1029/2001JE001505

Craddock, R. A., Maxwell, T. A., & Howard, A. D. (1997). Crater morphometry and modification in the Sinus Sabaeus and Margaritifer Sinus regions of Mars. *Journal of Geophysical Research*, *102*(E6), 13,321–13,340. https://doi.org/10.1029/97JE01084

Davis, J. M., Balme, M., Grindrod, P. M., Williams, R. M. E., & Gupta, S. (2016). Extensive Noachian fluvial systems in Arabia Terra: Implications for early martian climate. *Geology*, *44*(10), 847–850. https://doi.org/10.1130/G38247.1

Davis, J.M., Williams, R.M.E., Quantin, C., Weitz, C.M., Edgar, L., Dromart, G., & Grindrod, P.M. (2017). Selecting the sweet spot: Sampling strategies at southwestern Melas basin. Paper presented at 3rd Mars 2020 Landing Site Workshop, Monrovia, CA.

Di Achille, G., & Hynek, B. M. (2010). Ancient ocean on Mars supported by global distribution of deltas and valleys. *Nature Geoscience*, *3*(7), 459–463. https://doi.org/10.1038/ngeo891

Dromart, G., Quantin, C., & Olivier, B. (2007). Stratigraphic architectures spotted in southern Melas Chasma, Valles Marineris, Mars. *Geology*, *35*(4), 363–366. https://doi.org/10.1130/G23350A.1

Ehlmann, B. L., & Edwards, C. S. (2014). Mineralogy of the martian surface. *Annual Review of Earth and Planetary Sciences*, *42*(1), 291–315. https://doi.org/10.1146/annurev-earth-060313-055024

El-Maarry, M. R., Watters, W., Mckeown, N. K., Carter, J., Dobrea, E. N., Bishop, J. L., et al. (2014). Potential desiccation cracks on Mars: A synthesis from modeling, analogue-field studies, and global observations. *Icarus*, *241*, 248–268. https://doi.org/10.1016/j.icarus.2014.06.033

Fassett, C. I., & Head, J. W. III (2008a). The timing of martian valley network activity: Constraints from buffered crater counting. *Icarus*, *195*(1), 61–89. https://doi.org/10.1016/j.icarus.2007.12.009

Fassett, C. I., & Head, J. W. III (2008b). Valley network-fed, open-basin lakes on Mars: Distribution and implications for Noachian surface and subsurface hydrology. *Icarus*, *198*(1), 37–56. https://doi.org/10.1016/j.icarus.2008.06.016

Gallagher, C., & Balme, M. (2015). Eskers in a complete, wet-based glacial system in the Phlegra Montes region, Mars. *Earth and Planetary Science Letters*, *431*, 96–109. https://doi.org/10.1016/j.epsl.2015.09.023

Gendrin, A., Mangold, N., Bibring, J., Langevin, Y., Gondet, B., Bonello, G., et al. (2005). Sulfates in martian layered terrains: The OMEGA/Mars Express view. *Science*, *307*(5715), 1587–1591. https://doi.org/10.1126/science.1109087

Goddard, K., Warner, N. H., Gupta, S., & Kim, J.-R. (2014). Mechanisms and timescales of fluvial activity at Mojave and other young martian craters. *Journal of Geophysical Research: Planets*, *119*, 604–634. https://doi.org/10.1002/2013JE004564

Goldspiel, J. (2000). Groundwater sapping and valley formation on Mars. *Icarus*, *148*(1), 176–192. https://doi.org/10.1006/icar.2000.6465

Goudge, T. A., Fassett, C. I., Head, J. W., Mustard, J. F., & Aureli, K. L. (2016). Insights into surface runoff on early Mars from paleolake basin morphology and stratigraphy. *Geology*, *44*(6), 419–422. https://doi.org/10.1130/G37734.1

Goudge, T. A., Milliken, R. E., Head, J. W., Mustard, J. F., & Fassett, C. I. (2016). Sedimentological evidence for a deltaic origin of the western fan deposit in Jezero crater, Mars and implications for future exploration. *Earth and Planetary Science Letters*, *458*, 357–365. https://doi.org/10.1016/j.epsl.2016.10.056

Grindrod, P. M., & Balme, M. R. (2010). Groundwater processes in Hebes Chasma, Mars. *Geophysical Research Letters*, *37*, L13202. https://doi.org/10.1029/2010GL044122

Grindrod, P. M., Warner, N. H., Hobley, D. E. J., Schwartz, C., & Gupta, S. (2017). Stepped fans and facies-equivalent phyllosilicates in Coprates Catena, Mars. *Icarus*, *307*, 260–280. https://doi.org/10.1016/j.icarus.2017.10.030

Grindrod, P. M., West, M., Warner, N. H., & Gupta, S. (2012). Formation of an Hesperian-aged sedimentary basin containing phyllosilicates and sulfates in Coprates Catena, Mars. *Icarus*, *218*(1), 178–195. https://doi.org/10.1016/j.icarus.2011.11.027

Grotzinger, J. P., Gupta, S., Malin, M. C., Rubin, D. M., Schieber, J., Siebach, K., et al. (2015). Deposition, exhumation, and paleoclimate of an ancient lake deposit, Gale crater, Mars. *Science*, *350*(6257), aac7575. https://doi.org/10.1126/science.aac7575

Hartmann, W. K., & Neukum, G. (2001). Cratering chronology and the evolution of Mars. *Space Science Reviews*, *96*(1/4), 165–194. https://doi.org/10.1023/A:1011945222010

Howard, A. D., Moore, J. M., & Irwin, R. P. (2005). An intense terminal epoch of widespread fluvial activity on early Mars: 1. Valley network incision and associated deposits. *Journal of Geophysical Research*, *110*, E12S14. https://doi.org/10.1029/2005JE002459

Hynek, B. M., Beach, M., & Hoke, M. R. T. (2010). Updated global map of Martian valley networks and implications for climate and hydrologic processes. *Journal of Geophysical Research*, *115*, E09008. https://doi.org/10.1029/2009JE003548

Hynek, B. M., & Phillips, R. J. (2003). New data reveal mature, integrated drainage systems on Mars indicative of past precipitation. *Geology*, *31*(9), 757–760. https://doi.org/10.1130/G19607.1

Irwin, R. P., Craddock, R. A., & Howard, A. D. (2005). Interior channels in martian valley networks: Discharge and runoff production. *Geology*, *33*(6), 489–492. https://doi.org/10.1130/G21333.1

Irwin, R. P., & Howard, A. D. (2002). Drainage basin evolution in Noachian Terra Cimmeria, Mars. *Journal of Geophysical Research*, *107*(E7), E75056. https://doi.org/10.1029/2001JE001818

Irwin, R. P., Howard, A. D., Craddock, R. A., & Moore, J. M. (2005). An intense terminal epoch of widespread fluvial activity on early Mars: 2. Increased runoff and paleolake development. *Journal of Geophysical Research*, *110*, E12S15. https://doi.org/10.1029/2005JE002460

Jakosky, B. M., Slipski, M., Benna, M., Mahaffy, P., Elrod, M., Yelle, R., et al. (2017). Mars' atmospheric history derived from upper-atmosphere measurements of $^{38}Ar/^{36}Ar$. *Science*, *355*(6332), 1408–1410. https://doi.org/10.1126/science.aai7721

Jaumann, R., Neukum, G., Behnke, T., Duxbury, T. C., Eichentopf, K., & Flohrer, J. (2007). The high-resolution stereo camera (HRSC) experiment on Mars Express: Instrument aspects and experiment conduct from interplanetary cruise through the nominal mission. *Planetary and Space Science*, *55*(7-8), 928–952. https://doi.org/10.1016/j.pss.2006.12.003

Kirk, R. L., Howington-Kraus, E., Rosiek, M. R., Anderson, J. A., Archinal, B. A., Becker, K. J., et al. (2008). Ultrahigh resolution topographic mapping of Mars with MRO HiRISE stereo images: Meter-scale slopes of candidate Phoenix landing sites. *Journal of Geophysical Research*, *113*, E00A24. https://doi.org/10.1029/2007JE003000

Kite, E. S., Michaels, T. I., Rafkin, S., Manga, M., & Dietrich, W. E. (2011). Localized precipitation and runoff on Mars. *Journal of Geophysical Research*, *116*, E10002. https://doi.org/10.1029/2010JE003783

Kraal, E. R., Asphaug, E., Moore, J. M., Howard, A., & Bredt, A. (2008). Catalogue of large alluvial fans in martian impact craters. *Icarus*, *194*(1), 101–110. https://doi.org/10.1016/j.icarus.2007.09.028

Laity, J. E., & Malin, M. C. (1985). Sapping processes and the development of theater-headed valley networks on the Colorado Plateau. *Geological Society of America Bulletin*, *96*(2), 203–217. https://doi.org/10.1130/0016-7606(1985)96<203

Lamb, M. P., Dietrich, W. E., Aciego, S. M., Depaolo, D. J., & Manga, M. (2008). Formation of Box Canyon, Idaho, by megaflood: Implications for seepage erosion on Earth and Mars. *Science*, *320*(5879), 1067–1070. https://doi.org/10.1126/science.1156630

Lamb, M. P., Howard, A. D., Johnson, J., Whipple, K. X., Dietrich, W. E., & Perron, J. T. (2006). Can springs cut canyons into rock? *Journal of Geophysical Research*, *111*, E07002. https://doi.org/10.1029/2005JE002663

Le Deit, L., Bourgeois, O., Mège, D., Hauber, E., Le Mouélic, S., Massé, M., et al. (2010). Morphology, stratigraphy, and mineralogical composition of a layered formation covering the plateaus around Valles Marineris, Mars: Implications for its geological history. *Icarus*, *208*(2), 684–703. https://doi.org/10.1016/j.icarus.2010.03.012

Levy, J. S., Marchant, D. R., & Head, J. W. (2010). Thermal contraction crack polygons on Mars: A synthesis from HiRISE, Phoenix, and terrestrial analog studies. *Icarus*, *206*(1), 229–252. https://doi.org/10.1016/j.icarus.2009.09.005

Liu, Y., & Catalano, J. G. (2016). Implications for the aqueous history of southwest Melas Chasma, Mars as revealed by interbedded hydrated sulfate Fe/Mg-smecite deposits. *Icarus*, *271*, 283–291. https://doi.org/10.1016/j.icarus.2016.02.015

Lucchitta, B. K. (2010). Lakes in Valles Marineris. In N. A. Cabrol, & E. A. Grin (Eds.), *Lakes on Mars*, (pp. 111–161). Elsevier Science. https://doi.org/10.1016/B978-0-444-52854-4.00005-2

Lucchitta, B. K., McEwen, A. S., Clow, G. D., Geissler, P. E., Singer, R. B., Schultz, R. A., & Squyres, S. W. (1992). The canyon system on Mars. In H. H. Kieffer, B. M. Jakosky, C. W. Snyder, & M. I. Matthews (Eds.), *Mars*, (pp. 453–492). Tuscon: University of Arizona Press.

Malin, M. C., Bell, J. F. III, Cantor, B. A., Caplinger, M. A., Calvin, W. M., Clancy, R. T., et al. (2007). Context Camera Investigation on board the Mars Reconnaissance Orbiter. *Journal of Geophysical Research*, *112*, E05S04. https://doi.org/10.1029/2006JE002808

Malin, M. C., & Edgett, K. S. (2003). Evidence for persistent flow and aqueous sedimentation on early Mars. *Science*, *302*(5652), 1931–1934. https://doi.org/10.1126/science.1090544

Mangold, N., Ansan, V., Masson, P., Quantin, C., & Neukum, G. (2008). Geomorphic study of fluvial landforms on the northern Valles Marineris plateau, Mars. *Journal of Geophysical Research*, *113*, E08009. https://doi.org/10.1029/2007JE002985

Mangold, N., Quantin, C., Ansan, V., Delacourt, C., & Allemand, P. (2004). Evidence for precipitation on Mars from dendritic valleys in the Valles Marineris area. *Science*, *305*(5680), 78–81. https://doi.org/10.1126/science.1097549

Martha, T. R., Jain, N., Vamshi, G. T., & Kumar, K. V. (2017). Evidences of early aqueous Mars: Implications on the origin of branched valleys in the Ius Chasma, Mars. *Planetary and Space Science*, *148*, 56–65. https://doi.org/10.1016/j.pss.2017.10.011

McEwen, A. S., Eliason, E. M., Bergstrom, J. W., Bridges, N. T., Hansen, C. J., Delamere, W. A., et al. (2007). Mars Reconnaissance Orbiter's High Resolution Imaging Science Experiment (HiRISE). *Journal of Geophysical Research*, *112*, E05S02. https://doi.org/10.1029/2005JE002605

McEwen, A. S., Malin, M. C., Carr, M. H., & Hartmann, W. K. (1999). Voluminous volcanism on early Mars revealed in Valles Marineris. *Nature*, *397*(6720), 584–586. https://doi.org/10.1038/17539

Metz, J. M., Grotzinger, J. P., Mohrig, D., Milliken, R., Prather, B., Pirmez, C., et al. (2009). Sublacustrine depositional fans in southwest Melas Chasma. *Journal of Geophysical Research*, *114*, E10002. https://doi.org/10.1029/2009JE003365

Michael, G. G. (2013). Planetary surface dating from crater size–frequency distribution measurements: Multiple resurfacing episodes and differential isochron fitting. *Icarus*, *226*(1), 885–890. https://doi.org/10.1016/j.icarus.2013.07.004

Michalski, J., & Niles, P. B. (2012). Atmospheric origin of martian interior layered deposits: Links to climate change and the global sulfur cycle. *Geology*, *40*(5), 419–422. https://doi.org/10.1130/G32971.1

Moore, J. M., & Howard, A. D. (2005). Large alluvial fans on Mars. *Journal of Geophysical Research*, *110*, E04005. https://doi.org/10.1029/2004JE002352

Moore, J. M., Howard, A. D., Dietrich, W. E., & Schenk, P. M. (2003). Martian layered fluvial deposits: Implications for Noachian climate scenarios. *Geophysical Research Letters*, *30*(24), 2292. https://doi.org/10.1029/2003GL019002

Murchie, S. L., Mustard, J. F., Ehlmann, B. L., Milliken, R. E., Bishop, J. L., McKeown, N. K., et al. (2009). A synthesis of martian aqueous mineralogy after 1 Mars year of observations from the Mars Reconnaissance Orbiter. *Journal of Geophysical Research*, *114*, E00D06. https://doi.org/10.1029/2009JE003342

Neukum, G., & Jaumann, R. (2004). The High Resolution Stereo Camera of Mars Express. In Wilson, A. (Eds.), *Mars Express: The scientific payload*, *European Space Agency Special Publication*, (ESA-SP 1240, pp. 17–35). Noordwijk, Netherlands: ESA Publication Division ESTEC. https://doi.org/10.1016/j.pss.2016.02.014.

Pain, C. F., Clarke, J. D., & Thomas, M. (2007). Inversion of relief on Mars. *Icarus*, *190*(2), 478–491. https://doi.org/10.1016/j.icarus.2007.03.017

Pelletier, J. D., & Baker, V. R. (2011). The role of weathering in the formation of bedrock valleys on Earth and Mars: A numerical modeling investigation. *Journal of Geophysical Research*, *116*, E11007. https://doi.org/10.1029/2011JE003821

Quantin, C., Allemand, P., Mangold, N., Dromart, G., & Delacourt, C. (2005). Fluvial and lacustrine activity on layered deposits in Melas Chasma, Valles Marineris, Mars. *Journal of Geophysical Research*, *110*, E12S19. https://doi.org/10.1029/2005JE002440

Quantin, C., Weitz, C.M., Williams, R.M.E., Dromart, G., Mangold, N. (2006). Paleo-lake in Melas Chasma (Valles Marineris) as a potential landing site for MSL. Paper presented at 1st MSL Landing Site Selection Workshop, Pasadena, CA.

Rice, M. S., Bell, J. F. III, Gupta, S., Warner, N. H., & Anderson, R. B. (2013). A detailed geologic characterization of Eberswalde crater, Mars. *Mars*, *8*, 15–59. https://doi.org/10.1555/mars.2013.0002

Rice, M. S., Gupta, S., Treiman, A. H., Stack, K. M., Calef, F., Edgar, L. A., et al. (2017). Geologic overview of the Mars Science Laboratory rover mission at the Kimberley, Gale crater, Mars. *Journal of Geophysical Research: Planets*, *122*, 2–20. https://doi.org/10.1002/2016JE005200

Roach, L. H., Mustard, J. F., Swayze, G., Milliken, R. E., Bishop, J. L., Murchie, S. L., & Lichtenberg, K. (2010). Hydrated mineral stratigraphy of Ius Chasma, Valles Marineris. *Icarus*, *206*(1), 253–268. https://doi.org/10.1016/j.icarus.2009.09.003

Rotto, S., & Tanaka, K.L. (1995). Geologic/geomorphic map of the Chryse Planitia region of Mars. (Map I-2441, scale 1:5,000,000). United States Geological Survey Miscellaneous Investigation.

Salese, F., Di Achille, G., Neesemann, A., Ori, G. G., & Hauber, E. (2016). Hydrological and sedimentary analyses of well-preserved paleofluvial-paleolacustrine systems at Moa Valles, Mars. *Journal of Geophysical Research: Planets*, *121*, 194–232. https://doi.org/10.1002/2015JE004891

Saunders, I., & Young, A. (1983). Rates of surface processes on slopes, slope retreat and denudation. *Earth Surface Processes and Landforms*, *8*(5), 473–501. https://doi.org/10.1002/esp.3290080508

Schultz, R. A. (1991). Structural development of Coprates Chasma and western Ophir Planum, Valles Marineris Rift, Mars. *Journal of Geophysical Research*, *96*(E5), 22,777–22,792. https://doi.org/10.1029/91JE02556

Singh P., Sarkar, R., Porwal, A., & Binita, P. (2017). The diverse channels networks of Juventae Chasma, Mars. Paper presented at 48th Lunar And Planetary Science Conference, The Woodlands, Texas. Abstract 2603.

Smith, D. G. (1983). Anastomosed fluvial deposits: Modern examples from western Canada. In J. D. Collinson, & J. Lewin (Eds.), *Modern and ancient fluvial systems*, (Vol. 6, pp. 155–168). Oxford, UK: Blackwell Publishing Ltd. https://doi.org/10.1002/9781444303773.ch12

Smith, D. G. (1986). Anastomosing river deposits, sedimentation rates and basin subsidence, Magdalena River, northwestern Colombia, South America. *Sedimentary Geology*, *46*(3-4), 177–196. https://doi.org/10.1016/0037-0738(86)90058-8

Smith, E., Zuber, M. T., Frey, V., Garvin, B., Muhleman, O., Pettengill, H., et al. (2001). Mars Orbiter Laser Altimeter: Experiment summary after the first year of global mapping of Mars. *Journal of Geophysical Research*, *106*(E10), 23,689–23,722. https://doi.org/10.1029/2000JE001364

Strahler, A. N. (1958). Dimensional analysis applied to fluvially eroded landforms. *Bulletin of the Geological Society of America*, *69*(3), 279–300. https://doi.org/10.1130/0016-7606(1958)69[279:DAATFE]2.0.CO;2

Tanaka, K.L., Skinner, J.A., Dohm, J.M., Irwin, R.P., Kolb, E.J., Fortezzo, C.M., et al. (2014). Geologic map of Mars. USGS Scientific Investigations Series (Map 3292, scale 1:20,000,000). https://doi.org/10.3133/sim3292

Van Dijk, M., Kleinhans, M. G., Postma, G., & Kraal, E. (2012). Contrasting morphodynamics in alluvial fans and fan deltas: Effect of the downstream boundary. *Sedimentology*, *59*(7), 2125–2145. https://doi.org/10.1111/j.1365-3091.2012.01337.x

Van Dijk, M., Postma, G., & Kleinhans, M. G. (2009). Autocyclic behaviour of fan deltas: An analogue experimental study. *Sedimentology*, *56*(5), 1569–1589. https://doi.org/10.1111/j.13653091.2008.01047.x

Warner, N. H., Gupta, S., Calef, F., Grindrod, P., Boll, N., & Goddard, K. (2015). Minimum effective area for high resolution crater counting of martian terrains. *Icarus*, *245*, 198–240. https://doi.org/10.1016/j.icarus.2014.09.024

Warner, N. H., Sowe, M., Gupta, S., Dumke, A., & Goddard, K. (2013). Fill and spill of giant lakes in the eastern Valles Marineris region of Mars. *Geology*, *41*(6), 675–678. https://doi.org/10.1130/G34172.1

Weitz, C. M., & Bishop, J. L. (2016). Stratigraphy and formation of clays, sulfates, and hydrated silica within a depression in Coprates Chasma, Mars. *Journal of Geophysical Research: Planets*, *121*, 805–835. https://doi.org/10.1002/2015JE004954

Weitz, C. M., Milliken, R. E., Grant, J. A., McEwen, A. S., Williams, R. M. E., & Bishop, J. L. (2008). Light-toned strata and inverted channels adjacent to Juventae and Ganges chasmata, Mars. *Geophysical Research Letters*, *35*, L19202. https://doi.org/10.1029/2008GL035317

Weitz, C. M., Milliken, R. E., Grant, J. A., McEwen, A. S., Williams, R. M. E., Bishop, J. L., & Thomson, B. J. (2010). Mars Reconnaissance Orbiter observations of light-toned layered deposits and associated fluvial landforms on the plateaus adjacent to Valles Marineris. *Icarus*, *205*(1), 73–102. https://doi.org/10.1016/j.icarus.2009.04.017

Weitz, C. M., Noe Dobrea, E., & Wray, J. J. (2015). Mixtures of clays and sulfates within deposits in western Melas Chasma, Mars. *Icarus*, *251*, 291–314. https://doi.org/10.1016/j.icarus.2014.04.009

Weitz, C. M., Parker, T. J., Bulmer, M. H., Anderson, F. S., & Grant, J. A. (2003). Geology of the Melas Chasma landing site for the Mars Exploration Rover mission. *Journal of Geophysical Research*, *108*, E128082. https://doi.org/10.1029/2002JE002022

Williams, R. M. E., Grotzinger, J. P., Dietrich, W. E., Gupta, S., Sumner, D. Y., Wiens, R. C., et al. (2013). Martian fluvial conglomerates at Gale crater. *Science*, *340*(6136), 1068–1072. https://doi.org/10.1126/science.1237317

Williams, R. M. E., Irwin, R. P., & Zimbelman, J. R. (2009). Evaluation of paleohydrologic models for terrestrial inverted channels: Implications for application to martian sinuous ridges. *Geomorphology*, *107*(3-4), 300–315. https://doi.org/10.1016/j.geomorph.2008.12.015

Williams, R.M.E., Malin, M.C., & Edgett, K.S. (2005). Remnants of the courses of fine-scale, precipitation-fed runoff streams preserved in the martian rock record. Paper presented at 36th Lunar and Planetary Science Conference, Houston, Texas. Abstract 1173.

Williams, R.M.E., & Weitz, C. M. (2009). Stratigraphic context for inverted channels on the plains north of Juventae Chasma: Implications for post-Noachian martian climate change. Paper presented at 36th Lunar and Planetary Science Conference, The Woodlands, Texas. Abstract 1935.

Williams, R. M. E., & Weitz, C. M. (2014). Reconstructing the aqueous history within the southwestern Melas basin, Mars: Clues from stratigraphic and morphometric analyses of fans. *Icarus*, *242*, 19–37. https://doi.org/10.1016/j.icarus.2014.06.030

Williams, R. M. E., Weitz, C.M., Grindrod, P.M., Davis, J., Quantin, C., & Dromart, G. (2014). In situ investigation of the Southwestern Melas Basin. Paper presented at 1st Mars 2020a Landing Site Workshop, Crystal City, VA.

Williams, R. M. E., Weitz, C.M., Grindrod, P.M., Davis, J., Quantin, C., & Dromart, G. (2015). Accessible regions of interest within southwestern Melas Basin for exploration and sample collection by the Mars 2020b Rover. Paper presented at 2nd Mars 2020 Landing Site Workshop, Arcadia, CA.

Witbeck, N.E., Tanaka, K.L., & Scott, D.H. (1991). Geologic map of the Valles Marineris region, Mars. United States Geological Survey Miscellaneous Investigations Series (Map I-2010, scale 1: 2,000,000).

Zernitz, E. R. (1932). Drainage patterns and their significance. *The Journal of Geology*, *40*(6), 498–521. https://doi.org/10.1086/623976

Zuber, M. T., Smith, D. E., Solomon, S. C., Muhleman, D. O., Head, J. W., Garvin, J. B., et al. (1992). The Mars Observer Laser Altimeter investigation. *Journal of Geophysical Research*, *97*(E5), 7781–7797. https://doi.org/10.1029/92JE00341